Theoretical proposals for the experimental detection of electrodynamic interactions between biomolecules

Matteo Gori, Elena Floriani, Pettini Marco

Theoretical proposals for the experimental detection of electrodynamic interactions between biomolecules

Matteo Gori*

Department of Physics and Sciences of Materials,

University of Luxembourg, Luxembourg and

Quantum Biology Lab, Howard University, 2400 6th St NW, Washington, DC 20059, USA

Elena Floriani† and Marco Pettini‡

Aix Marseille Univ, Université de Toulon, CNRS, CPT, Marseille, France and

CNRS Centre de Physique Théorique UMR7332, 13288 Marseille, France

(Dated: June 17, 2021)

Abstract

The present work follows a series of investigations of ours aimed at understanding whether long-range intermolecular electrodynamic forces could play a role in accelerating the encounter of the cognate partners of biochemical reactions in living matter and by which experimental methods and available techniques these forces could be detected. After the experimental detection of collective intramolecular oscillations of protein molecules [that we reported in Phys. Rev.X8, 031061 (2018)] the possibility of observing the mentioned electrodynamic interactions appears more realistic and thus deserving a deeper theoretical investigation of possible experimental detection of these forces with new data at hand.

*Electronic address: gori6matteo@gmail.com

†Electronic address: floriani@cpt.univ-mrs.fr

‡Electronic address: marco.pettini@cpt.univ-mrs.fr;corresponding_author

I. INTRODUCTION

From the physics point of view, one of the most striking and challenging problem arising from molecular biology stems from the observation that biochemical reactions - which commonly involve a huge number of actors - are coordinated simultaneously to be achieved in due time, thus granting the reality of well organized dynamic systems. The spatial dimensions of these systems are much larger than the "action radii" of chemical reactions, of electrostatic and quasi-electrostatic interactions (which are strongly shielded both by the large static value of water dielectric constant and by freely moving ions), and of van der Waals-London dispersion interactions. Yet the interactions between cognate molecular partners in living matter (eg, nucleic acids and transacting nuclear proteins; cytoskeleton and signaling membrane proteins, etc..) produce a highly specific and efficient spatial-temporal biochemical pattern of encounters, which can hardly be explained by taking into account random diffusion only. A longstanding proposal [1–4] surmised that the encounters of distant cognate partners of biomolecular reactions could be actively driven by selective (resonant) attractive forces of electrodynamic nature. The implications of an experimental confirmation of the actual activation of electrodynamic interactions among biomolecules could have a revolutionary impact on our understanding of the functioning of the molecular machinery at work in living matter. This would open new avenues of fundamental research in biophysics, both theoretical and experimental. We have revisited Fröhlich's proposal [5] and started a series of studies [6–9] aimed at understanding how these forces could be detected experimentally. We recently made two important experimental steps forward, the first consisted in checking how the diffusion properties of biomolecules in solution can be affected by long-range interactions, and this was successfully tested by means of Fluorescence Correlation Spectroscopy (FCS) with built-in long-range forces (electrostatic ones) [10]. The second major leap forward was the excitation and detection through THz spectroscopy of a Fröhlich-like phonon condensation occurring in BSA proteins under external energy pumping [11], this second achievement paves the way to the possibility of activating the above mentioned intermolecular electrodynamic forces [4, 5]. In what follows we shall thoroughly investigate two different physical phenomena that can be univocally affected by the activation of long-range electrodynamic interactions. We shall explicitly refer to the BSA protein and to R-PE (Red-Phycoerythrin) protein, the former already studied in [11] and the latter

under investigation by the same research group in which the authors of the present paper participate. Also the R-PE molecules have been found to undergo collective oscillations under external energy pumping.

II. EFFECTS OF ELECTRODYNAMIC INTERACTIONS ON MOLECULAR DIFFUSION

In this section we introduce three different theoretical and numerical models in order to predict the possible outcomes of FCS experiments on the BSA or R-PE proteins that are expected to undergo a clustering transition [7]. In the following, we provide quantitative predictions concerning the occurrence of experimental outcomes of this kind due to the presence of long range dipole-dipole electrodynamic intermolecular interactions.

Some simplifications are assumed to define a model that can be studied at least semi-analytically. We are interested in the behaviour determined by long-range interactions for values of the R-PE concentration in solution such that the intermolecular average distance is much larger than the characteristic size of the molecule. For this reason the particles are considered as spherical in our models. All the spheres are assumed to have the same radius. The radius of the spherical particles has been chosen such that their volume is equivalent to the volume $\mathcal{V}_{\rm RPE}$ of the R-PE estimated from the mass $M_{\rm RPE} \approx 2.5 \times 10^2$Da,

$$a = \left(\frac{3}{4\pi} \frac{M_{\rm RPE}}{\rho_{\rm BM}} \right)^{1/3} \simeq 42\,\text{Å} \tag{1}$$

where the density of the biomolecule has been set to $\rho_{\rm BM} = 1.27\ \ \mathrm{g\,cm^{-3}}$ [12][13] .

A. The effective potential

The interaction potential among resonant oscillating electric dipoles is supposed to take the effective form

$$U_{\rm eff}(r_{ij}) = -\frac{3 c_{\rm eff} k_B T R_0^3}{r_{ij}^3 + 2R_0^3} \tag{2}$$

where $r_{ij} = \|\boldsymbol{r}_j - \boldsymbol{r}_i\|$ is the distance between the i-th and j-th molecules, k_B is the Boltzmann constant, T is the temperature and R_0 is a length scale. The form of the potential in Eq.(2)

has been chosen such that

$$U_{\text{eff}}(R_0) = c_{\text{eff}} k_B T \quad \text{and} \quad U''_{\text{eff}}(R_0) = 0 \ . \tag{3}$$

The regularization in the denominator has been introduced in order to avoid the divergence in $\|\mathbf{r}_i - \mathbf{r}_j\| = 0$. The parameter R_0 has been chosen to be the sum of two molecular radii $R_0 = 2a = 84\,\text{Å}$. The strength of the potential in $k_B T$ units at the distance R_0 between the particle centers is given by the parameter c_{eff} which can hardly be assessed *a priori*. The dynamical electric dipole moment can be estimated by equating the effective potential with the quasi-static dipole-dipole interaction energy

$$U_{dd}(r_{ij}) \simeq -\frac{p^2}{4\pi\varepsilon_0\varepsilon_W(\omega) r_{ij}^3} \tag{4}$$

at the distance $r_{ij} = r_*$, i.e. $U_{dd}(r_*) = U_{\text{eff}}(r_*)$. The relative dielectric constant of the medium is assumed to be $\varepsilon_W(\omega) = |\varepsilon(\omega_{\text{CVM}})|$, where the suffix CVM stands for Collective Vibrational Motion, the relation between the strength of the potential and the electric dipole moment of the biomolecules is given by $p = \alpha(r_*, T) c_{\text{eff}}^{1/2}$, where the calibration constant α depends on the distance r_* at which the two potentials are set equal and T is the temperature. The results for different choices of T and r_* are reported in Table I for R-PE ($\nu_{\text{CVM}} = 71\,\text{GHz}$).

r_*[Å]	$T[K]$	$\alpha[D]$
82	293	7.10×10^2
950	293	1.23×10^3
82	303	1.25×10^3
950	303	1.30×10^3

TABLE I: Different values of the factor α.

B. Semi-Analytical Model

The discussion of this semi-analytical model is adapted from an analogous calculation for the clustering transition in a self-gravitating system [14] where the long-range attractive interaction potential among particles scales with the distance r as r^{-1}. The model developed in this section aims at verifying the possible existence of a clustering transition in the FCS experiments when the translation degrees of freedom of the molecules are at thermal equilibrium and the interparticle electrodynamic interaction potential scales as r^{-3}. The experimental setting is represented in a simplified way as a system of N spherical particles of radius $a = 42\,\text{Å}$ confined in a sphere of radius R of volume equal to the FCS confocal effective volume as defined in [15]

$$V_{\text{eff}} = (2)^{3/2} V_{\text{conf}} = \pi^{3/2} w_0^2 z_0 \ . \tag{5}$$

In real experiments two typical sizes w_0 and z_0 can be assumed to be $w_0 = 2.8 \times 10^3$Å and $z_0 = 5w_0 = 1.4 \times 10^4$Å, yielding a volume-equivalent spherical system of radius

$$R = \left(\frac{3\pi^{1/2}}{4} w_0^2 z_0 \right)^{1/3} \simeq 5.265 \times 10^3 \text{Å} \tag{6}$$

The configuration of a system of N particles is in principle described by the probability density function in configuration space $\rho_N(\mathbf{r}_1, ..., \mathbf{r}_N)$. In the simplified model here considered, the volume, the temperature and the number of molecules inside the volume are fixed so that the thermodynamic equilibrium is defined as the probability distribution that minimizes the free energy functional $F[\rho_N](N, V, T)$

$$F[\rho_N](N, V, T) = U[\rho_N] - TS[\rho_N] \ . \tag{7}$$

where $U[\rho_N]$ is the average potential energy

$$U[\rho_N] = \int_{\mathcal{S}^3(R)} \mathrm{d}^3\mathbf{r}_1 ... \int_{\mathcal{S}^3(R)} \mathrm{d}^3\mathbf{r}_N \ U(\mathbf{r}_1, ...\mathbf{r}_N) \rho_N(\mathbf{r}_1, ..., \mathbf{r}_N) \tag{8}$$

while the entropy $S[\rho_N]$ is defined as

$$S[\rho_N] = -\int_{\mathcal{S}^3(R)} \mathrm{d}^3\mathbf{r}_1 ... \int_{\mathcal{S}^3(R)} \mathrm{d}^3\mathbf{r}_N \;\; \rho_N(\mathbf{r}_1, ..., \mathbf{r}_N) \log\left[\rho_N(\mathbf{r}_1, ..., \mathbf{r}_N)\right] \; . \tag{9}$$

The distribution $\rho_{N,\mathrm{eq}}$ such that $\delta F[\rho_{N,\mathrm{eq}}]/\delta\rho_N = 0$ and $\delta^2 F[\rho_{N,\mathrm{eq}}]/\delta\rho_N^2 > 0$ corresponds to the probability distribution at thermodynamic equilibrium in the canonical ensemble. We point out that such a description does not coincide with the real experimental setting because in FCS experiments the particles can freely enter into and exit out of the confocal volume, so that the hypothesis of a fixed number of particles holds only in the average. The control parameter in real experiments is the concentration of biomolecules, or, equivalently, the *intermolecular average distance* $\langle d \rangle$: in our model this corresponds to a different choice of the number of molecules in the total volume

$$N(\langle d \rangle) = \left\lfloor \frac{4\pi}{3} \left(\frac{R}{\langle d \rangle} \right)^3 \right\rfloor \tag{10}$$

where $\lfloor \cdot \rfloor$ is the floor operator. It is convenient to introduce adimensionalized quantities, choosing the effective radius as the length scale of the model so that $\widetilde{R} = R/a \simeq 1.25 \times 10^2$.

We consider a *mean field approximation* for the probability density distribution of the biomolecules in the volume, i.e.

$$\rho_N(\mathbf{r}_1, ..., \mathbf{r}_N) = \prod_{i=1}^{N} \rho_1(\mathbf{r}_i) \tag{11}$$

We make the following ansatz about the functional form of $\rho_1(\mathbf{r})$, i.e.

$$\begin{aligned} \rho_1(\widetilde{\mathbf{r}}, \eta) &= \eta\Theta(\widetilde{R}_*(\eta) - \|\widetilde{\mathbf{r}}\|)\rho_c(\mathbf{r}) + (1-\eta)\Theta(\|\widetilde{\mathbf{r}}\| - \widetilde{R}_*(\eta))\Theta(\widetilde{R} - \|\widetilde{\mathbf{r}}\|)\rho_h(\mathbf{r}) = \\ &= \eta\Theta(\widetilde{R}_*(\eta) - \|\widetilde{\mathbf{r}}\|)\frac{3}{4\pi\widetilde{R}_*^3(\eta)} + (1-\eta)\Theta(\|\widetilde{\mathbf{r}}\| - \widetilde{R}_*(\eta))\Theta(\widetilde{R} - \|\widetilde{\mathbf{r}}\|)\frac{3}{4\pi\left[\widetilde{R}^3 - \widetilde{R}_*^3(\eta)\right]} \end{aligned} \tag{12}$$

which means that a particle is found with probability η in a spherical cluster of radius R_* located at the center of the ambient spherical space. The radius of the cluster is determined by considering the random close packing for spheres $g = 0.637$ (maximum volume fraction

for a randomly packed 3D system) such that

$$\widetilde{R}_*(\eta, \langle d \rangle) = R_*/a = \sqrt[3]{g^{-1}\eta N(\langle d \rangle)} \tag{13}$$

where a is the effective radius of the considered molecules in the cluster, taking into account all short range interactions (dispersive forces, hydrodynamic forces, etc.). In what follows, we denote by a tilde superscript the adimensionalized length expressed in units of the particles radius a.

Remark. *The mean field approximation and the form of the one-particle distribution in Eq.*(12) *is a sort of "fluid approximation": the more the volume of the particles is negligible with respect to the total volume, the better the approximation.*

An estimation of the excluded volume effects is provided by the following parameter

$$\gamma(\langle \tilde{d} \rangle, \widetilde{R}) = \left\{ \frac{\prod_{i=1}^{N(\langle \tilde{d} \rangle, \tilde{R})} [V - (i-1)4\pi a^3/3]}{V^{N(\langle \tilde{d} \rangle, \tilde{R})}} \right\}^{\frac{1}{N(\langle \tilde{d} \rangle, \tilde{R})}} = \sqrt[N(\langle \tilde{d} \rangle, \tilde{R})]{\prod_{i=1}^{N(\langle \tilde{d} \rangle, \tilde{R})} \left[1 - (i-1)\widetilde{R}^{-3}\right]} \tag{14}$$

In the limit of large $\widetilde{R}$, γ is a function only of the (adimensionalized) intermolecular average distance, in fact

$$\begin{aligned} \log \gamma &= \frac{1}{N(\langle \tilde{d} \rangle, \tilde{R})} \sum_{i=1}^{N(\langle \tilde{d} \rangle, \tilde{R})} \log \left[1 - (i-1)\widetilde{R}^{-3}\right] \approx -\frac{\widetilde{R}^{-3}}{N(\langle \tilde{d} \rangle, \tilde{R})} \sum_{i=1}^{N(\langle \tilde{d} \rangle, \tilde{R})} (i-1) = \\ &= \frac{1}{2} \frac{\left[N(\langle \tilde{d} \rangle, \tilde{R}) - 1\right]}{\widetilde{R}^3} \approx -\frac{2\pi}{3\langle \tilde{d} \rangle^3} + \frac{1}{2\tilde{R}^3} \approx -\frac{2\pi}{3\langle \tilde{d} \rangle^3} = \log \gamma_{app} \ . \end{aligned} \tag{15}$$

As a first approximation, we can assume that in the FCS experiments the degrees of freedom relative to the centers of the biomolecules are at thermal equilibrium, and that the number of particles in the confocal volume is constant. These assumptions allow to tackle the system of interacting biomolecules in the canonical ensemble framework. The adimensional specific free energy functional is defined as

$$\frac{F[\rho_N]}{N k_B T} = \frac{U[\rho_N]}{N k_B T} - \frac{S[\rho_N]}{k_B N} = u[\rho_N] - s[\rho_N] \ . \tag{16}$$

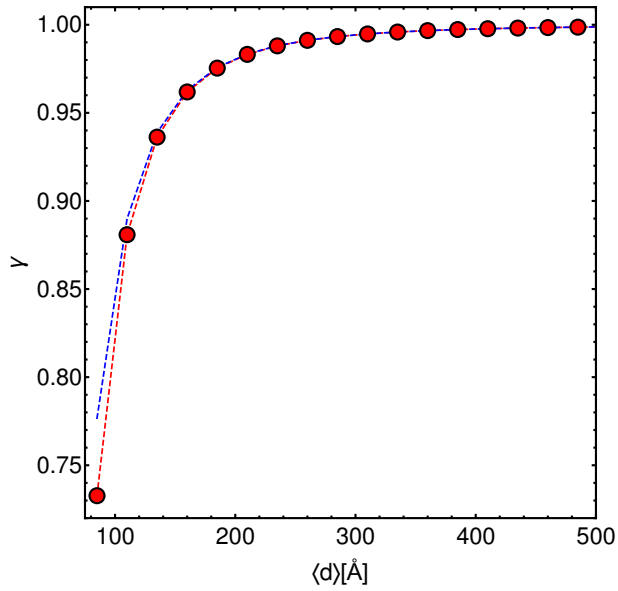

FIG. 1: Effective accessible volume γ, for intermolecular distances $\langle d \rangle$ in the range $90 \div 600$ Å. In red circles the numerical values of γ calculated using the exact expression in Eq.(14), the blue line representing the data obtained using the approximated function. In this case, the effective radius of the molecule is $a = 42$ Å and the radius relative to the total volume $R = 5246$ Å.

The (adimensional) specific entropy $s[\rho_N]$ is given by

$$s[\rho_N] = \frac{S[\rho_N]}{N k_B} = -\frac{1}{N} \int_{\mathbb{S}^3(\widetilde{R})} \rho_N \ \log \rho_N \ \prod_{i=1}^{N} \mathrm{d}r_i^3 \ . \tag{17}$$

and substituting Eq.(12) in the previous expression we obtain

$$s(\eta, \langle d \rangle) = s[\rho_N] = -\left[\eta \log \left(\frac{3\eta}{4\pi \widetilde{R}_*^3(\eta, \langle d \rangle)} \right) + (1-\eta) \log \left(\frac{3(1-\eta)}{4\pi(\widetilde{R}^3 - \widetilde{R}_*^3(\eta, \langle d \rangle))} \right) \right] \ . \tag{18}$$

The expected specific potential energy $u[\rho_N]$ is given by three separate contributions:

$$u[\rho_N] = u_{\mathrm{c-c}}[\rho_N] + u_{\mathrm{c-h}}[\rho_N] + u_{\mathrm{h-h}}[\rho_N] \tag{19}$$

the self-interaction of the molecules contained in the central cluster

$$u_{c-c}(\eta, \langle d \rangle) = u_{c-c}[\rho_N] = -\eta^2 \frac{N(\langle d \rangle) - 1}{2} \int_{\mathcal{S}(\widetilde{R}_*)} \mathrm{d}^3 \widetilde{r}_i \int_{\mathcal{S}(\widetilde{R}_*)} \mathrm{d}^3 \widetilde{r}_j \ \rho_c(\widetilde{\mathbf{r}}_i) \rho_c(\widetilde{\mathbf{r}}_j) \frac{24 c_{\mathrm{eff}}}{\|\widetilde{\mathbf{r}}_i - \widetilde{\mathbf{r}}_j\|^3 + 16}, \tag{20}$$

the interaction among the halo and the cluster

$$u_{c-h}(\eta,\langle d\rangle)=u_{c-h}[\rho_N]=-\eta(1-\eta)\quad\frac{N(\langle d\rangle)-1}{2}\times\int_{\mathcal{S}(\widetilde{R}_*)}\mathrm{d}^3\widetilde{r}_i\int_{\mathcal{C}(\widetilde{R},\widetilde{R}_*)}\mathrm{d}^3\widetilde{r}_j\ \rho_c(\widetilde{\mathbf{r}}_i)\rho_h(\widetilde{\mathbf{r}}_j)\frac{24c_{\text{eff}}}{\|\widetilde{\mathbf{r}}_i-\widetilde{\mathbf{r}}_j\|^3+16},\tag{21}$$

and the self-interaction of the halo

$$u_{h-h}(\eta,\langle d\rangle)=u_{h-h}[\rho_N]=-(1-\eta)^2\frac{N(\langle d\rangle)-1}{2}\times\int_{\mathcal{C}(\widetilde{R},\widetilde{R}_*)}\mathrm{d}^3\widetilde{r}_i\int_{\mathcal{C}(\widetilde{R},\widetilde{R}_*)}\mathrm{d}^3\widetilde{r}_j\ \rho_h(\widetilde{\mathbf{r}}_i)\rho_h(\widetilde{\mathbf{r}}_j)\frac{24c_{\text{eff}}}{\|\widetilde{\mathbf{r}}_i-\widetilde{\mathbf{r}}_j\|^3+16}\ .\tag{22}$$

where $\mathcal{S}(x)$ is a sphere with radius x centered at the origin and $\mathcal{C}(x,x')$ is a spherical shell centered at the origin and with external and internal radii x and x' respectively. The fraction of clustered molecules at equilibrium is obtained by minimizing the specific free energy with respect to η at fixed $\langle d\rangle$, i.e.

$$\eta_{\min}(\langle d\rangle)=\left\{\eta\in[0,1]\,|\,F(\eta_{\min})=\min_{\eta\in[0,1]}\frac{F(\eta,\langle d\rangle)}{N(\langle d\rangle)k_BT}\quad\text{for any fixed }\langle d\rangle\right\}\ .\tag{23}$$

As it can be observed in Figure 2, there exists a range of values of the effective dipole-dipole potential strength c_{eff} such that the specific free energy $F/(Nk_BT)$ has a relative minimum for a certain value of the clustered fraction $\eta'\in(0,1)$, for any fixed value of the intermolecular average distance $\langle d\rangle$. In these cases, the value of the relative minimum of the specific free energy decreases with the intermolecular average distance $\langle d\rangle$. This means that it is possible to find a value of the parameter c_{eff} such that $F(\eta')<F(0)$. In our case, we have empirically found that by setting $c_{\text{eff}}=0.325$, it is $F(\eta')\lesssim F(0)$ for $\langle d\rangle\lesssim 950\,\text{Å}$ (see Figure 2). Moreover, almost all the molecules are in the clustered phase as $\eta'=\eta_{\min}>0.93$ for $c_{\text{eff}}=0.325$ and $\langle d\rangle\lesssim 950\,\text{Å}$ (see Figure 2), while for $\langle d\rangle\gtrsim 975\,\text{Å}$ the equilibrium of the system is in the disperse phase. We conclude that long range attractive interactions scaling as r^{-3} with the intermolecular distance r can induce an experimentally observable clustering phase transition. According to Table I the estimated value of the dynamic dielectric dipole is $|\mathbf{p}|=400\div 740\text{D}$. We remark that such a value constitutes an underestimation of the real dynamical dielectric dipole because the electrodynamic interactions can be either

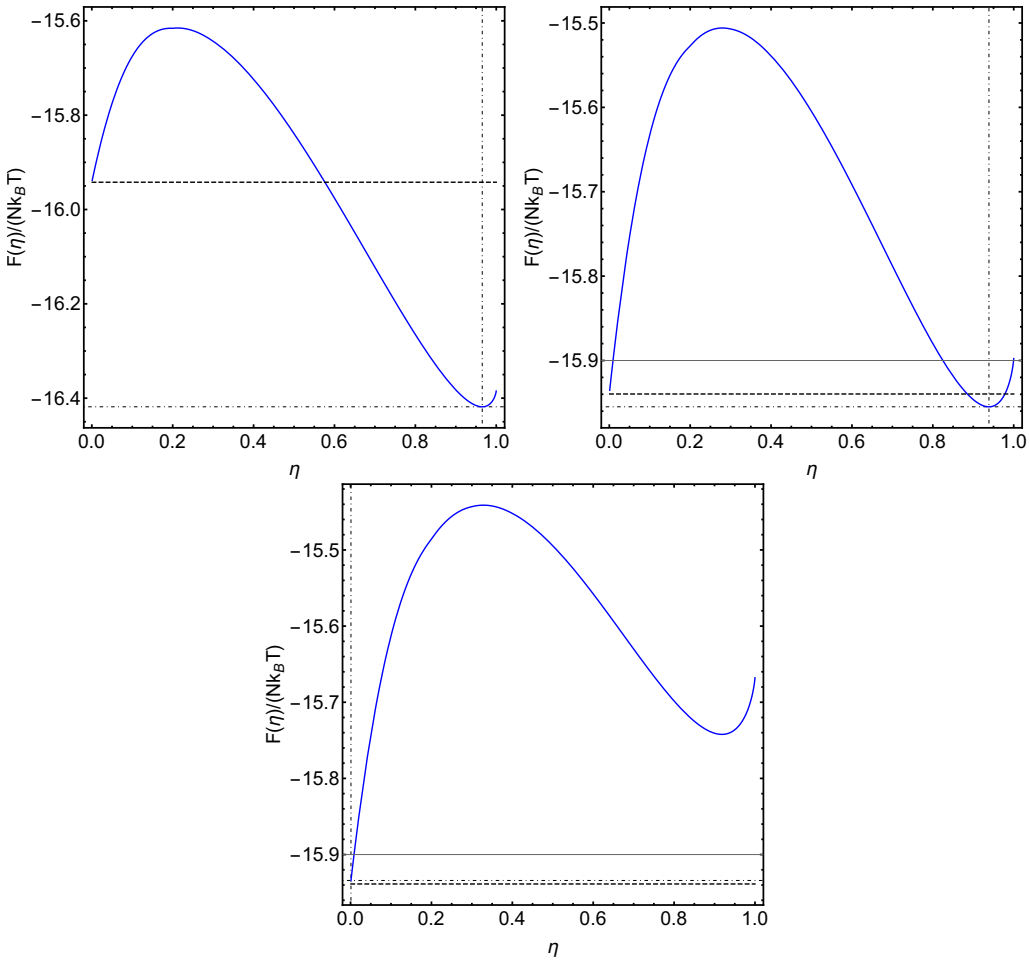

FIG. 2: Specific free energy $F/(k_BTN)$ vs. clustered fraction η for different values of the intermolecular average distance $\langle d\rangle$ at $c_{\rm eff} = 0.325$. Upper left panel : $\langle d\rangle = 900\,$Å; upper right panel: $\langle d\rangle = 950\,$Å; lower panel: $\langle d\rangle = 975\,$Å.

attractive or repulsive, and this depends on the mutual oscillation phase and orientation of the dipoles, whereas in the mean field model considered in this section, the interactions are always attractive.

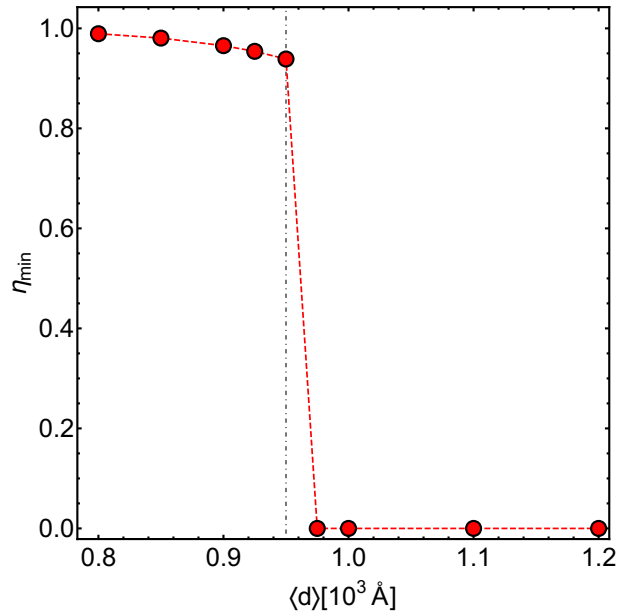

FIG. 3: Clustered fraction η as a function of the intermolecular average distance $\langle d \rangle$ for a system of particles interacting through the potential in Eq.(2) with $c_{\text{eff}} = 0.325$. $\eta_{min} \simeq 1$ corresponds to the clustered phase whereas $\eta_{min} \simeq 0$ corresponds to the dispersed (gaseous) phase.

C. Molecular Dynamics Study of the clustering transition

Molecular dynamics simulations have been done in order to estimate the effect of long-range electrodynamic interactions, described by the effective potential in Eq.(2), on the self-diffusion coefficient D of a system of interacting molecules defined by

$$D = \lim_{t \to +\infty} \frac{\langle \|\Delta \mathbf{r}_i(t)\|^2 \rangle_i}{6t} \tag{24}$$

where $\Delta \mathbf{r}_i(t)$ is the displacement at time t of the i-th molecule with respect to its initial position, and $\langle \cdot \rangle_i$ is the average over all the particles in the system. This is the physical quantity measured by means of FCS experiments thus allowing a direct comparison between the outcomes of numerical simulations and the outcomes of lab experiments.

We considered a system made of a fixed cubic box of volume equal to the effective volume in Eq.(5), hence of side $L = (V_{\text{eff}})^{1/3} = 8486\,\text{Å}$. Given an intermolecular distance $\langle d \rangle$, the corresponding number of particles in the box is determined through Eq.(10).

The dynamics is given by the Langevin equations in the overdamped limit (without

inertial terms):

$$\frac{\mathrm{d}\mathbf{r}_i}{\mathrm{d}t} = -\frac{1}{\gamma}\nabla_{\mathbf{r}_i}\sum_{j\neq i} U(\|\mathbf{r}_i - \mathbf{r}_j\|) + \sqrt{\frac{2k_BT}{\gamma}}\boldsymbol{\xi}_i(t) \qquad \forall i = 1,..,N \tag{25}$$

where γ is the viscous friction constant, T is the temperature of the solution and $\boldsymbol{\xi}_i(s)$ is a noise term, s.t.

$$\langle \xi_{A,i}(t)\rangle_t = 0 \quad \langle \xi_{A,i}(t)\xi_{B,j}(t')\rangle_t = \delta(t-t')\delta_{AB}\delta_{i,j} \qquad \forall i,j = 1,...,N \quad \forall A,B = 1,...,3\ . \tag{26}$$

As we have assumed that the molecules are represented by spherical particles, we use Stokes' formula for the viscous friction constant of a sphere in a viscous fluid, i.e.

$$\gamma = \frac{1}{6\pi R_H \eta_W(T)} \tag{27}$$

where R_H is the hydrodynamic radius in water and $\eta_W(T)$ is the dynamical viscosity of water at the temperature T. As we are more interested in a qualitative rather than a quantitative description of the diffusive dynamics and of the clustering transition, we can reasonably assume that $R_H = a = 42\,\text{Å}$ while the water dynamical viscosity as a function of temperature at the atmospheric pressure is estimated using the following formula [16]

$$\eta_W(T) = A\exp[B/(T-C)] \tag{28}$$

where $A = 2.407\times10^{-5}\text{Pa}\cdot\text{sec}$, $B = 571.5\,\text{K}$ and $C = 139.7\,\text{K}$. The water dynamical viscosity is $\eta(T_{\text{exp}}) = 0.7915\times10^{-3}\,\text{Pa}\cdot\text{sec}$ at the experimental value $T_{\text{exp}} = 30\,^{\circ}\text{C} = 303.15\,\text{K}$, according to Eq.(28). The potential energy used for these molecular dynamics simulations is given by

$$U(r) = \begin{cases} U_{\text{eff}}(r) + U_{\text{Debye}}(r) & r > 2(1.01)a \\ U_{SC}(r) & r \leq 2(1.01)a \end{cases} \tag{29}$$

where U_{eff} is the effective potential energy of Eq.(2) due to electrodynamic interactions.

U_{Debye} is the Debye potential [17] due to electrostatic interactions

$$U_{\text{Debye}}(r) = \frac{Z^2 e^2 \exp\left[-\dfrac{r}{\lambda_D}\right]}{4\pi\varepsilon_0\varepsilon_W(1+R/\lambda_D)r}\,. \tag{30}$$

Here Z is the net charge of the molecule, e is the electric charge of the electron, ε_0 is the vacuum permittivity, ε_W is the water relative dielectric constant and λ_D is the Debye length

$$\lambda_D = \left(\frac{\sum_i \rho_{\infty,i} e^2 z_i^2}{\varepsilon_0\varepsilon_W k_B T}\right)^{-1/2}\,, \tag{31}$$

where $\rho_{\infty,i}$ is the concentration of the i-th electrolyte species and T is the temperature of the solution. In our case, this results in a Debye length $\lambda_D \approx 9.74\,\text{Å}$. The net charge for R-PE molecules has been fixed to $Z = +10$.

The effect of Pauli's repulsion among the electronic clouds of molecules is described through a Buckingham-like soft core potential U_{SC}

$$U_{SC}(R) = A_{SC}\exp\left(-\frac{r}{\lambda_{\text{B}}}\right) \tag{32}$$

where $\lambda_{\text{B}} = 2a$. The parameter A_{SC} fixing the strength of the potential has been chosen such that if the molecules overlap for the 10% of their radii they are brought back to be tangent to one another, i.e.

$$\|\Delta_{SC}\mathbf{x}_1 + \Delta_{SC}\mathbf{x}_2| = \frac{2\|\mathbf{F}_{sc}(1.9\,a)\|}{\gamma}\Delta t = 0.1\,a \tag{33}$$

yielding

$$A_{SC} = 0.05\gamma a\exp\left[-0.95\right] \approx 1.93\times 10^{-3}\frac{\gamma a}{\Delta t}\,. \tag{34}$$

A soft-core potential has been preferred with respect to an hard-core potential because the latter would require a very small integration time step (i.e. of the same order as in all-atoms simulations, $10^{-12}s$) to avoid nonphysical large displacements. Moreover, using a very small time step would be at odds with the hypothesis of overdamped Brownian dynamics. And the dynamics would require a prohibitively large number of time steps. Periodic boundary conditions have been assumed for the positions of the particles but not

for the long-range interactions that are computed without taking into account the images of the particles (due to the periodic boundary conditions). This latter choice is due to the fact that the long range electrodynamic interactions are supposed to be active only for particles in the effective volume of FCS, simulated by the cubic box.

The numerical simulations have been performed using the Heun predictor-corrector algorithm with a time step $\Delta t = 5 \times 10^{-4} \mu$s and for a total number of steps $N_{\rm steps} = 2 \times 10^7$, corresponding to a total simulation time $T_{\rm tot} = 10^4 \mu$s. In order to assess the adequacy of this integration time, let us first notice that with the present choice of parameters the Brownian diffusion coefficient of the spherical molecules in simulations is $D = k_B T \gamma^{-1} = k_B T (6\pi a \eta_W)^{-1} \simeq 6.68 \times 10^3 \text{Å}^2 \mu\text{s}^{-1}$. Then considering a sphere circumscribing the box, thus of radius $R_{\rm circ} = \sqrt{3} l/2 \simeq 7.35 \times 10^3$Å, the characteristic time scale expected for a molecule to explore all the volume is $t_{\rm Vol} = R_{\rm circ}^2/(6D) \simeq 1.35 \times 10^3 \mu$s, largely contained in the total integration time of $10^4 \mu$s.

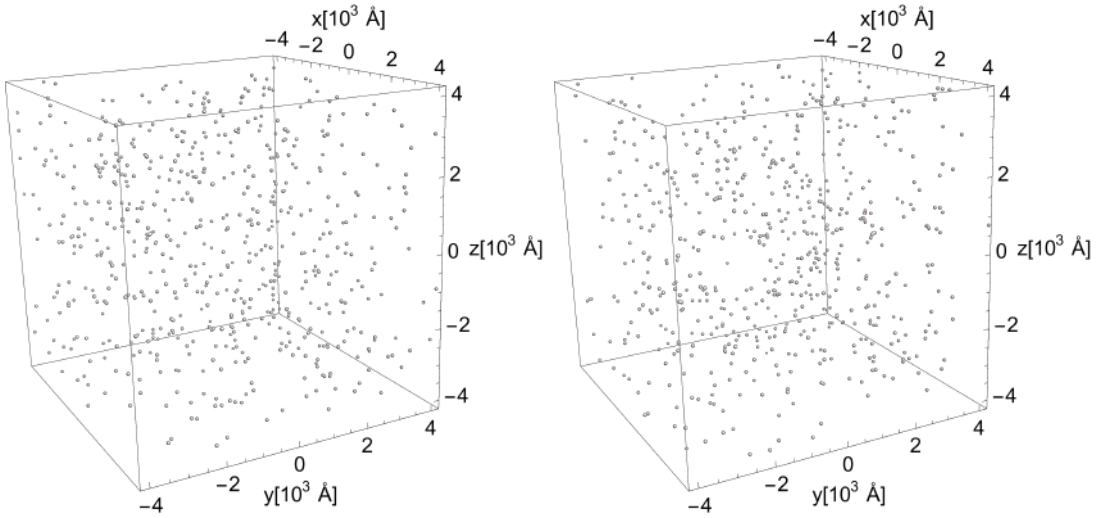

FIG. 4: Molecular dynamics simulations. Snapshots of spatial distributions of 500 molecules corresponding to an intermolecular average distance of $\langle d \rangle = 1000$ Å. Left box: the initial condition. Right box: the final configuration after $10^4 \mu$s.

Molecular Dynamics simulations of equations (25) yield the results for the diffusion coefficient D, normalized by the Brownian value D_0, reported in Figure 6 as a function of the average intermolecular distance $\langle d \rangle$. The sudden drop of D/D_0 is a clear effect of the clustering phase transition. The same pattern of D/D_0 versus $\langle d \rangle$ is displayed by the experimental outcomes of FCS experiments reported in Figure 3 of the Main text.

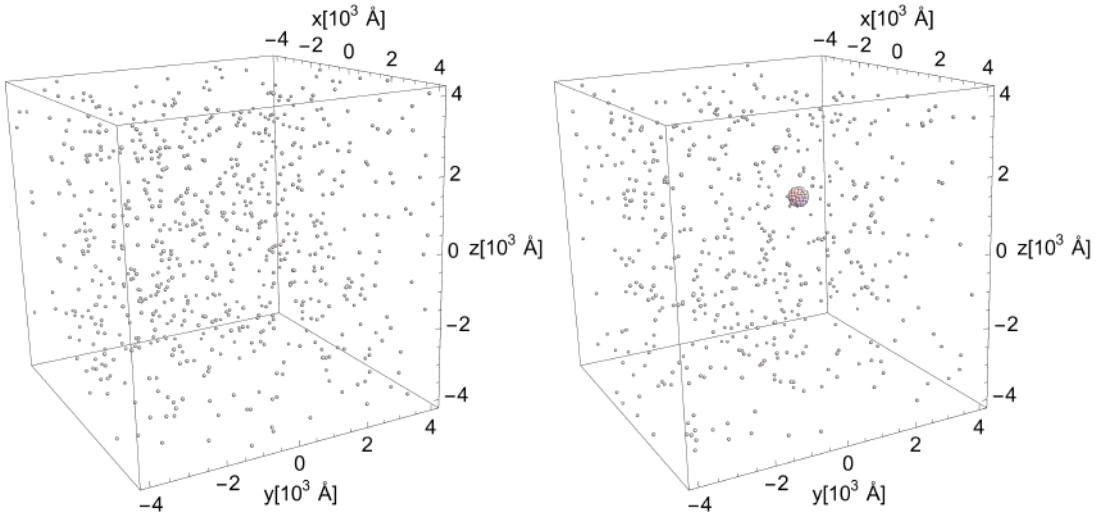

FIG. 5: Molecular dynamics simulations. Snapshots of spatial distributions of 700 molecules corresponding to an intermolecular average distance of $\langle d \rangle = 950\,\text{Å}$. Left box: the initial condition. Right box: the final configuration after $10^4 \mu$s.

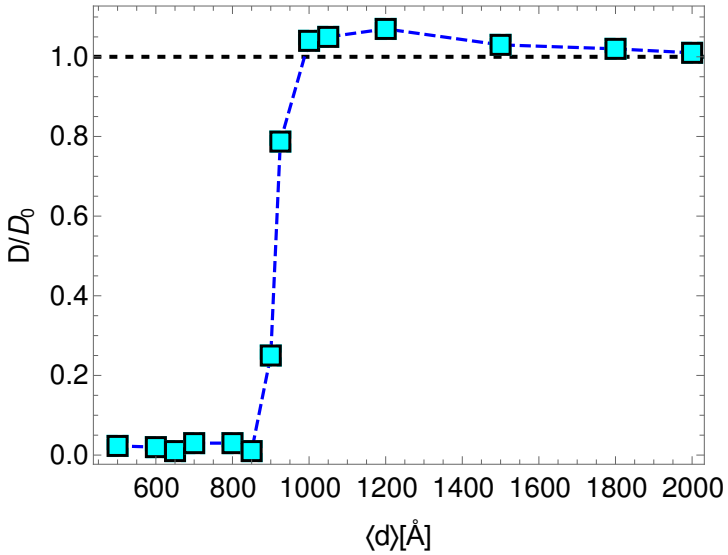

FIG. 6: Relative self diffusion coefficient D/D_0 vs. intermolecular average distance $\langle d \rangle$ for a system of mutual interacting particles in a cubic box of size length $L = 8486\,\text{Å}$ and the strength of the dipole interaction potential fixed at $c_{\text{eff}} = 2.25$.

D. MonteCarlo simulations for the clustering transition

Equation (2) provides a first rough approximation of the electrodynamic potential derived in Ref.[5] for the interaction among two oscillating electric dipoles, as it does not take into account their mutual orientation nor their relative oscillation phase. At first, taking into account these degrees of freedom results in an interaction potential of indefinite sign, i.e.

the long-range electrodynamic force between oscillating biomolecules can be attractive or repulsive as well. Therefore, it is important to check whether or not the clustering transition takes place also in presence of an orientation-dependent dipole-dipole interaction. If this is the case, we need to determine the value of the oscillating electric dipole moment that is necessary to explain prospective experimental observations, that is, the value of $\langle d \rangle$ at which the clustering transition is expected. To achieve this aim, Monte Carlo simulations have been performed.

1. Potential Energy

In order to have a better approximation of the interaction, the following form for the potential energy is considered:

$$U_{\mathrm{Tot}}(\mathbf{p}_i, \mathbf{p}_j, \mathbf{r}_{ij}) = \begin{cases} +\infty & r_{ij} < 2a \\ U_{\mathrm{Hmk}}(r_{ij}) + U_{\mathrm{Dby}}(r_{ij}) + U_{\mathrm{EDdip}}(\mathbf{p}_i, \mathbf{p}_j, \mathbf{r}_{ij}) & r_{ij} \geq 2a \end{cases} \tag{35}$$

where $\mathbf{r}_{ij}$ is the vector joining the centers of the i-th and the j-th molecule, U_{Dby} is the screened electrostatic potential of the force exerted between net charges of biomolecules, U_{EDdip} is the electrodynamic potential between resonant oscillating giant dipoles and U_{Hmk} is the pairwise Hamacker dispersive interaction energy. In more details:

- the electrostatic screened potential due to the presence of counterions has the form of the Debye-Hückel potential [17] $U_{\mathrm{Debye}}(r)$ in eq. (30) with the same choice of parameters;

- the Hamacker potential energy describes dispersive interactions among extended spherical bodies and takes the form [17]

$$U_{\mathrm{Hmk}}(r) = -\frac{A}{6}\left[\frac{2R_1R_2}{(2R_1+2R_2+r)r} + \frac{2R_1R_2}{(2R_1+r)(2R_2+r)} + \right. \\ \left. + \ln\frac{(2R_1+2R_2+r)r}{(2R_1+r)(2R_2+r)}\right] \tag{36}$$

  where $A = 3 - 10\ k_BT$ is the typical value of the *Hamacker constant* for proteins [18, 19], and R_i is the radius of the i-th particle. In our simulations the Hamacker

constant has been set to $A = 10\,k_B T$ with the radii $R_1 = R_2 = a = 42\,\text{Å}$.

- The electrodynamic interaction is assumed to be pairwise and of the form

$$U_{\text{EDdip}}(\mathbf{p}_i, \mathbf{p}_j, \mathbf{r}_{ij}) = f_{\text{reg}}(r_{ij}) \frac{\mathbf{p}_i \cdot \mathbf{p}_j - 3(\mathbf{p}_i \cdot \hat{\mathbf{r}}_{ij})(\mathbf{p}_j \cdot \hat{\mathbf{r}}_{ij})}{4\pi\varepsilon_0 \varepsilon_W(\omega_{\text{CVM}}) r_{ij}^3} \tag{37}$$

where $\mathbf{p}_i$ is the *dynamical* electric dipole moment of the i-th molecule, $\hat{\mathbf{r}}_{ij} = \mathbf{r}_{ij}/r_{ij}$ is the unit vector directed from the i-th particle to j-th one. The details of the derivation of this potential will be provided in Section III A.

The interaction energy of a system of oscillating dipoles is generally speaking a function of time. Nevertheless, following the derivation in [5], the interaction energy has been averaged *over a time scale much larger than the typical period of dipole oscillation.* In so doing, the interaction energy depends only on the position of the dipoles, their orientations and their relative phase of oscillation $\Delta\alpha_{ij} = \alpha_j - \alpha_i$. The effect of this relative phase can be included in the relative orientation of the dipoles, so that the system of interacting oscillating resonant dipoles is mapped into a system of static dipoles. A regularization provided by the function $f_{reg}(r_{ij})$ has been introduced to make the electrodynamic potential smoothly smeared out for $r \longrightarrow R_0 = 2a$ and equivalent to the non regularized potential at infinity, i.e. $\lim_{r\to+\infty} f_{\text{reg}}(r) = 1$. To comply with these requirements, the regularizing function is chosen of the form

$$f_{\text{reg}}(r) = -\tanh\left(\frac{R_0 - r}{R_0 \sigma_{\text{reg}}}\right) . \tag{38}$$

where the parameter $\sigma_{\text{reg}} = 0.679$ is determined after the assumption that $f_{\text{reg}}(2R_0) = 0.9$ (see Figure 7 for the effect of the regularization over a generic potential $U(r) = -r^{-3}$). The introduction of this regularization is physically motivated on the one side by the short distance repulsion of molecular electron clouds due to the Pauli exclusion principle, and on the other side by the imaginable hydrodynamic friction effects that could dump the collective oscillations responsible for electrodynamic interactions.

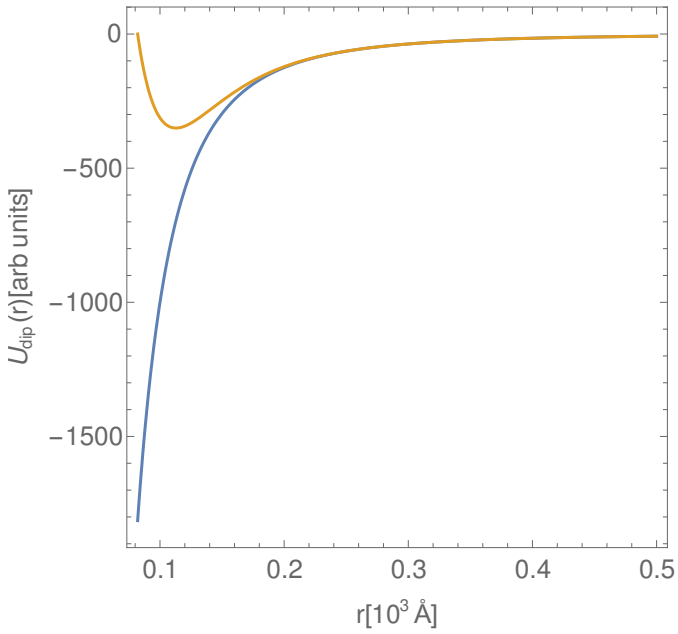

FIG. 7: Effects of the damping function $f_{\rm reg}(r)$ on a potential $U = -r^{-3}$. In blue the non regularized potential $-r^{-3}$, in orange the regularized potential $U_{\rm reg}(r) = f_{\rm reg}(r)U(r)$.

2. *Details of the simulations*

The simulations have been performed by considering a cubic box of side $L = 8486\,\text{Å}$, with spherical particles of radius $a = 42\,\text{Å}$. As for the molecular dynamics simulations described in Section II C, the dimensions of the fixed simulation box are chosen so that $V_{\rm eff} = L^3$, and the number of particles in the box is changed in order to vary the intermolecular average distance $\langle d \rangle$, i.e.

$$N = \left\lfloor \frac{L^3}{V_{\rm eff}} \right\rfloor \tag{39}$$

The degrees of freedom updated by the Monte Carlo Dynamics are the three Cartesian coordinates (x_i, y_i, z_i) and the polar angles (ϕ_i, θ_i) defining the position of the center of mass and the orientation of the dynamical electric dipole of each molecule, respectively. The domain for the coordinates of the center of mass is defined by $x_i, y_i, z_i \in [0, L]$ and $\phi \in [0, 2\pi)$, $\theta \in [0, \pi]$ for the angular coordinates. The m-th Monte Carlo step is performed according to the Metropolis algorithm prescriptions. In a system consisting of N particles, N random extractions of a particle are performed. At the k-th extraction of the m-th step, a test configuration $\{(\tilde{\mathbf{x}}_{i_k}(m), \tilde{\phi}_{i_k}(m), \tilde{\theta}_{i_k}(m)\}$ is created for the chosen particle labeled by i_k through a random displacement in configuration space with respect to a reference

configuration, i.e.

$$\begin{cases} \tilde{\mathbf{x}}_{i_k}(m) = \mathbf{x}_{i_k}(m-1) + \Delta x \;\; \boldsymbol{\xi}_{i_k}(m) \\ \tilde{\phi}_{i_k}(m) = \phi_{i_k}(m-1) + \Delta\phi \;\; \xi_{\phi,i_k}(m) \\ \tilde{\theta}_{i_k}(m) = \theta_{i_k}(m-1) + \Delta\theta \;\; \xi_{\theta,i_k}(m) \end{cases} \tag{40}$$

where each $\xi_{\alpha,i}(m)$ is a Gaussian-distributed random variable with zero mean and unit variance:

$$\langle \xi_{\alpha,i}(m)\xi_{\beta,j}(m+m')\rangle = \delta_{m',0}\delta_{i,j}\delta_{\alpha,\beta} \tag{41}$$

where the average $\langle\cdot\rangle$ is intended over many realizations of the random process. The probability to accept a trial configuration is given by

$$T_{x\to\tilde{x}} = \min\left\{\frac{\exp[-\beta V(\tilde{x})]}{\exp[-\beta V(x)]}, 1\right\}. \tag{42}$$

If the trial configuration is accepted and a particle exits from the box, it is reinjected into the volume using the following prescription: the distance of the center of the particle from the box is calculated as:

$$d_i = \sqrt{\sum_{k=1}^{3}\left[x_{k,i}^2\Theta(-x_{k,i}) + (x_{k,i}-l)^2\Theta(x_{k,i}-l)\right]}, \tag{43}$$

then the particle is reinjected into the box at a distance d_i from a randomly chosen side of the box. More precisely, two random numbers η_1, η_2 are chosen in the interval $[0, L]$ and a third random number η_{sel} is extracted in order to determine the reinjection side, i.e. if $\mathbf{x}_i$ are the coordinates of the reinjected particle:

$$\mathbf{x}_i = \begin{cases} (d_i, \eta_1, \eta_2) & \text{for} \quad 0 \geq \eta_{sel} > 1/6 \\ (L-d_i, \eta_1, \eta_2) & \text{for} \quad 1/6 \geq \eta_{sel} > 1/3 \\ (\eta_1, d_i, \eta_2) & \text{for} \quad 1/3 \geq \eta_{sel} > 1/2 \\ (\eta_1, L-d_i, \eta_2) & \text{for} \quad 1/2 \geq \eta_{sel} > 2/3 \\ (\eta_1, \eta_2, d_i) & \text{for} \quad 2/3 \geq \eta_{sel} > 5/6 \\ (\eta_1, \eta_2, L-d_i) & \text{for} \quad 5/6 \geq \eta_{sel} > 1\,. \end{cases} \tag{44}$$

This particular choice for the boundary conditions has been made in order to mimic the continuous flow of particles in and out of the confocal volume taking place in FCS experiments. As long-range interactions are assumed to be activated by the blue light only in the confocal volume and to be absent outside it, no correction of the long-range electrodynamic potential is needed (this would be in general the case with long range interactions requiring corrections to account for the contributions of the images of the system due to periodic boundary conditions).

3. Results of the simulations

The simulations have been performed choosing random positions and orientations for the particles in the box which represents the confocal volume. The number of Monte Carlo steps has been fixed to $N_{\mathrm{MCsteps}} = 2\times10^6$ with $\delta_x = \Delta x/a = 2$ and $\delta_{\mathrm{ang}} = \Delta\theta/\pi = \Delta\phi/(2\pi) = 0.1$.

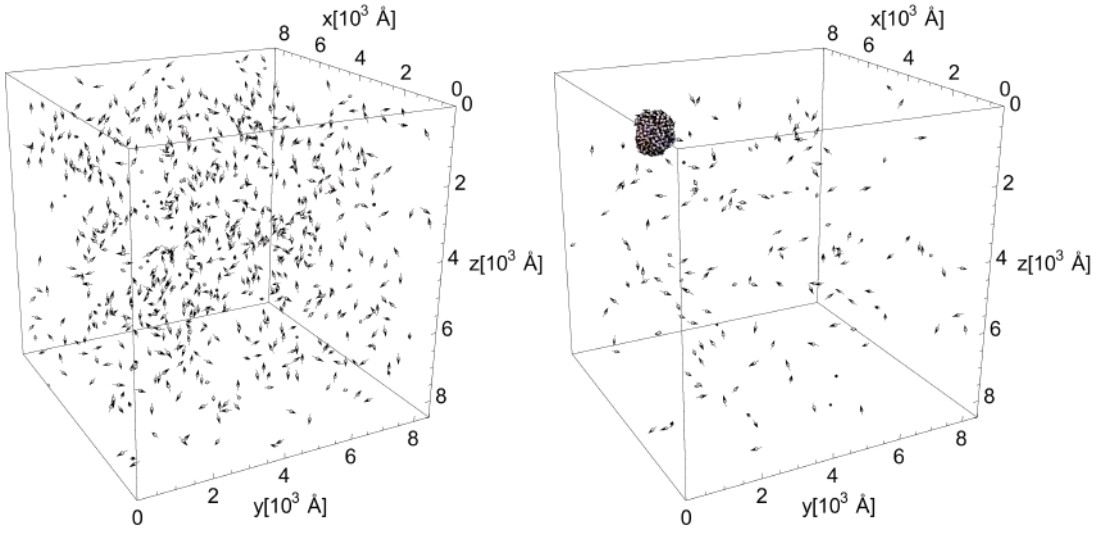

FIG. 8: Clustering transition: snapshots corresponding to the clustered phase in a cubic system of side $L = 8486\,\text{Å}$, with intermolecular average distance $\langle d\rangle = 950\,\text{Å}$, obtained by setting the number of particles to $N = 713$ and the dynamic electric dipole to $|\mathbf{p}| = 2900D$ at $T = 303.15K = 30\,^{\circ}\text{C}$. Left box: the initial condition. Right box: the final configuration after 2×10^6 Montecarlo steps.

This makes the square root of the mean square displacement of each particle $\sqrt{\mathrm{MSD}} \approx \sqrt{3}\Delta x\sqrt{2\times10^6} \approx 2.05\times10^5\text{Å} \approx 24L$, that is, large enough. In order to optimize the convergence rate of the dynamics to the stationary state of the system, an adaptive method has been introduced. Each 10^2 Monte Carlo steps the running acceptance ratio η_{AR} is calculated: if $\eta_{\mathrm{AR}} < 0.33$ the relative displacements $\delta_x, \delta_{\mathrm{ang}}$ are halved (up to 5 times) while

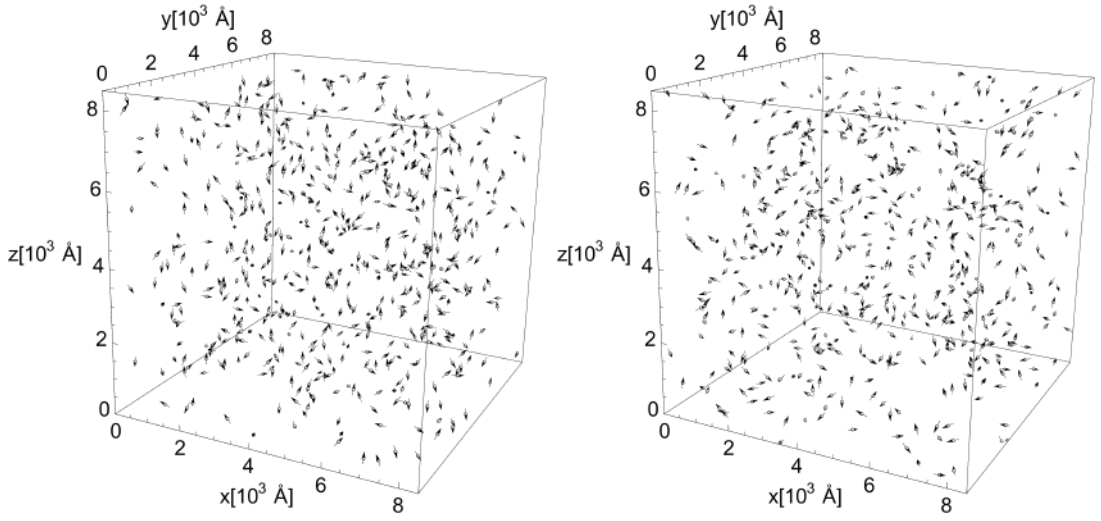

FIG. 9: Absence of clustering: snapshots of the disperse phase in a cubic system of side $L = 8486\,\text{Å}$, with intermolecular average distance $\langle d \rangle = 1000\,\text{Å}$, obtained by setting the number of particles to $N = 611$ and the dynamic electric dipole to $|\mathbf{p}| = 2900D$ at $T = 303.15K = 30\,^{\circ}\text{C}$. Left box: the initial condition. Right box: the final configuration after 2×10^6 Montecarlo steps.

if $\eta_{\text{AR}} > 0.85$ the relative displacements are doubled one time. The results reported in Figures 8 and 9 correspond to a value $|\mathbf{p}| = 2900\,\text{D}$ of the modulus of the dynamic electric dipolar momentum. This value of $|\mathbf{p}|$ has been found to produce a clustering transition for $\langle d \rangle \lesssim 950\,\text{Å}$ (see Figure 8) that disappears for $\langle d \rangle \gtrsim 1000\,\text{Å}$ (see Figure 9).

III. EFFECTS OF ELECTRODYNAMIC INTERACTIONS ON THE FREQUENCY OF MOLECULAR COLLECTIVE VIBRATIONS

A. Preliminaries

In THz spectroscopy experiments, the absorption peaks corresponding to collective intramolecular vibrations of both R-PE and BSA proteins can be expected to undergo a frequency shift [9] proportional to molecular concentration.

In [11] it has been argued that these absorption peaks are the spectroscopic signature of a classical Fröhlich condensation-like phenomenon, i.e. when the energy injection rate exceeds a threshold value the energy pumped into a molecule is almost entirely channelled into its lowest frequency mode, and this entails a collective vibration of the whole molecule. Recently, it has been suggested that a full and deeper understanding of the experimental results reported in [11] requires a quantum treatment of the Fröhlich condensation mecha-

nism (see [20]). Even if this proposal is very interesting and robust, for the purposes of the present work we can proceed in the conceptual framework of a classical description.

In what follows, a biomolecule of mass M is represented by two spheres, each one of mass $M_{\rm crg} = M/2$ (where crg stands for center of charge) and effective charge $Z_{\rm eff}$, connected by a spring of elastic constant $k_{\rm CVM} = M\omega_{\rm CVM}^2/4$, where $\omega_{\rm CVM} = 2\pi\nu_{\rm CVM}$ is the characteristic angular frequency of a collective vibrational mode (CVM).

The spring is actually a doughnut-like extended elastic object (the R-PE protein) mainly made of α-helices each one behaving like a spring. In its extension modes, because of geometric constraints, we can reasonably assume that the velocity of each mass element of the molecule is larger at the external parts and lower at the interior. A common assumption is a linear dependence of the velocity of a mass element passing from the slower part to the faster part. This means that the velocity u of a mass element dM is taken as $u(r) = vr/R$, where R is the larger radius of the molecule and r is the radial coordinate from the center. Assuming a uniform mass distribution we have $dM = M\ dr/R$. The kinetic energy of the molecule then reads

$$K = \int_{molecule} \frac{1}{2}u^2(r)dM(r) = \frac{Mv^2}{2R^3}\int_0^R r^2 dr = \frac{1}{2}\frac{M}{3}v^2$$

where M is the rest mass of the molecule and $M/3$ (known as the Rayleigh limit) is the effective mass contributing to the kinetic energy of the spring consisting of an extended elastic object.

Due to the Equipartition Theorem, at thermodynamic equilibrium the amplitude Δx of the oscillations of the charge barycenters around the equilibrium position is given by

$$k_B T = M_{\rm eff}\ \omega_{\rm CVM}^2 \langle(\Delta x)^2\rangle \Rightarrow \quad \sigma_{\Delta x,Th} = \sqrt{\langle(\Delta x)^2\rangle} = \frac{1}{2\pi\nu_{\rm CVM}}\sqrt{\frac{k_B T}{M_{\rm eff}}} = \frac{7.99\times10^{-2}\text{Å}}{[\nu_{\rm CVM}]\sqrt{[M_{\rm eff}]}} \tag{45}$$

where $M_{\rm eff} = M_{crg}/6 = M/12$, the experimental temperature is assumed $T = 30\,^{\circ}\text{C} = 303.15K$, the frequency $[\nu_{\rm CVM}]$ is expressed in THz and the reduced mass $[M_{\rm eff}]$ is expressed in KDa. For R-PE the observed peak of lowest frequency is at $[\nu_{\rm CVM}] = 0.71 \times 10^{-1}$ and $[M_{\rm eff}] \simeq 20$, so that the amplitude of the oscillation is $\sigma_{\Delta x} \approx 2.5\times10^{-1}$Å. For BSA, the observed collective vibrational mode is $[\nu_{\rm CVM}] = 3.14 \times 10^{-1}$ and the characteristic mass $[M_{\rm eff}] \simeq 5.5$ so that the expected relative distance between the charge barycenters is

$\sigma_{\Delta x} \approx 1.85 \times 10^{-2}$Å.

The R-PE has a strong absorption at $\lambda_{\mathrm{AB,RPE}} \simeq 488\,\mathrm{nm}$ and the emission peak is around $\lambda_{EM,RPE} \simeq 580\,\mathrm{nm}$: it follows that for a number n_{flc} of fluorochromes the quantity of energy absorbed is

$$\begin{aligned} &\Delta E_{\mathrm{RPE}} < \eta\ n_{\mathrm{flc}} hc(\lambda^{-1}_{\mathrm{AB,RPE}} - \lambda^{-1}_{\mathrm{EM,RPE}}) \simeq \\ &\simeq \eta\ n_{\mathrm{flc}} \times 15.4 \times (k_B\, 303.15\,\mathrm{K}) \simeq \eta\ n_{\mathrm{flc}} \times 6.457 \times 10^{-13}\mathrm{erg}\ , \end{aligned} \tag{46}$$

where η is the efficiency of the energy transfer from the fluorochrome to mechanical vibrational (phonon) modes of the biomolecule. The description of the details of such a process goes far beyond the purpose of this paper, but an efficiency around 10% can be expected (for further details on a possible mechanism describing the conversion of electronic excitation into mechanical excitation see [21]). It follows that the maximum extension amplitude for the oscillating molecules is estimated to be:

$$\sigma_{\Delta x,Fc} = \sqrt{\langle (\Delta x)^2 \rangle} < \frac{1}{2\pi\nu_{\mathrm{CVM}}} \sqrt{\frac{\eta(n_{\mathrm{flc}} \times 15.4) \times k_B T}{M_{\mathrm{eff}}}} \simeq \sqrt{\eta\ n_{\mathrm{flc}}} \times 5.6 \times 10^{-1}\text{Å} \tag{47}$$

assuming for R-PA $n_{\mathrm{flc}} = 38$ and $\eta = 0.1$ we obtain $\sigma_{\Delta x,Fc} \approx 1.08\,$Å. The activation of a coherent excitation due to Fröhlich-like condensation is represented in the simple model here considered as a phase-defined oscillation maintained for a coherence time $\tau_{cohr} \gg \nu^{-1}_{\mathrm{CVM}}$. So we can assume that the time evolution of the distance between the charge barycenters is given by

$$x_i(t) = x_{0,i} + \frac{1}{2}\left\{x_{\omega,i} \exp[-\mathrm{i}(\omega_{\mathrm{CVM}} t + \phi_i)] + c.c\right\}\ , \tag{48}$$

where $x_{\omega_0,i} = \sqrt{2}\sigma_{\Delta x}$ and ω_{CVM} is the angular frequency of oscillation of the single molecule in the limit of high dilution. In real experiments with R-PE, the Q-factor of the absorption peak at the resonant frequency can be expected in the range $50 \div 90$, so the coherence time can be estimated through:

$$\tau_{cohr}\nu_{\mathrm{CVM}} \approx \frac{Q}{\pi} \approx 16 \div 30 \Rightarrow \tau_{cohr} \approx \frac{Q}{\pi\nu_{\mathrm{CVM}}} \approx 2.2 \div 4.0 \times 10^{-1}\mathrm{ns} \tag{49}$$

Considering the possibly largest experimentally expected (at high temperature) diffusion coefficient of R-PE $D_0 \approx 250\,\mu\mathrm{m}^2\mathrm{s}^{-1}$ the displacement of the particle during the interval of

coherent oscillations is of the order

$$\sqrt{\langle|\Delta\mathbf{r}_i|^2\rangle} \approx \sqrt{6D_0\tau_{cohr}} \approx 5.8 \div 8 \text{ Å} \tag{50}$$

which is much less than the intermolecular average distance and the characteristic dimension of the protein.

In this limit we can consider the positions and the orientations of the molecules as fixed for a time t_{int} such that $\tau_{cohr} \geq t_{\text{int}} \gg \nu_{\text{CVM}}^{-1}$. We can assume that the electric dipole of a single molecule in a reference frame attached to the molecule takes the form

$$\begin{aligned} \mathbf{p}_i(t) \simeq \mathbf{p}_{\text{stat},i} + \mathbf{p}_{\text{dyn},i}(t) = \left\{ p_0 + \frac{p_\omega}{2} \exp\left[-\mathrm{i}(\omega t + \phi_i)\right] + c.c. \right\} \hat{\mathbf{p}}_i = \\ = Z_{\text{eff}} e \left\{ x_0 + \frac{x_\omega}{2} \exp\left[-\mathrm{i}(\omega t + \phi_i)\right] + c.c. \right\} \hat{\mathbf{p}} \qquad x_0, x_\omega \in \mathbb{R}^+ \end{aligned} \tag{51}$$

where $\hat{\mathbf{p}}$ is the normal vector that indicates the direction of the dipole, Z_{eff} can be defined as the equivalent charge of a symmetric dipole, i.e.

$$Z_{\text{eff}} = Z_+ - \frac{Z_{\text{Tot}}}{2} = Z_- + \frac{Z_{\text{Tot}}}{2} \tag{52}$$

and the relative position $\mathbf{x}$ of the charge barycenters is defined by

$$\mathbf{p}(t) = Z_+\mathbf{r}_+(t) + Z_-\mathbf{r}_-(t) = Z_{\text{eff}}\mathbf{x}(t)\,. \tag{53}$$

If the value of the effective separated charge is $Z_{\text{eff}}\, e$ then the electric dynamic dipole has the following maximum

$$p_{\omega_{\text{CVM}}} = Z_{\text{eff}}\, e\, \sigma_{\Delta x} < Z_{\text{eff}} \times \sqrt{\eta n_{\text{flc}}} \times 2.69\,\text{D}\ . \tag{54}$$

It is known that the charge barycenters of biomolecules are separated by a distance of $\sim 3 \div 10$ Å [22], one order of magnitude larger than the estimated $x_{\omega_{\text{CVM}}}$. However, we can argue that in an electrolytic solution with a Debye length comparable to that of living cells, that is $\lambda_{\text{D}} \approx 10\,\text{Å}$, the interaction due to the electrostatic charge distribution is negligible with respect to the electrodynamic interactions between the dynamical parts $\mathbf{p}_{\text{dyn},i}(t)$ of the oscillating dipoles of two distinct molecules.

1. The electrodynamic interactions among the oscillating dipoles

According to [5] the large dipole oscillations induced by energy injection and subsequent Fröhlich condensation are responsible for long-range interactions between biomolecules. Let us consider a system of N identical molecules, such that each molecule has a total mass M and a net charge $Z_{\rm net}$ and can be represented as a system of two lumps of mass $M_{\rm eff} = M/2$ and connected by an harmonic spring of elastic constant $k = M_{\rm eff}\,\omega_{\rm CVM}^2$. The dynamical variables are the distances among the charge barycenters, $x_i(t) = x_{0,i} + x_{{\rm dyn},i}(t)$ so that the dipole moment can be written $\mathbf{p}_i(t) = Z_{\rm eff} x(t) e\hat{\mathbf{p}}_i$. As the measured frequency shift due to the interactions is expected to be a perturbation we can assume that the vibrational mode with an angular frequency very close to $\omega_{\rm CVM}$ has been activated, i.e.

$$x_i(\omega) \neq 0 \qquad \text{only if } |\omega \pm \omega_{\rm CVM}| < \epsilon\omega_{\rm CVM} \quad \text{for } \epsilon \ll 1 \tag{55}$$

If we consider the systems on a characteristic time scale τ_{int} such that $\tau_{cohr} \geq \tau_{int} \gg \nu_{\rm CVM}^{-1}$, we can ignore the dissipation in the oscillation of the dipoles, and the total energy of the system for the vibrational degrees of freedom can be written as

$$\begin{aligned} H_{\rm dipOs}(\boldsymbol{P}_i(t), \mathbf{x}_i(t)) = \sum_{i=1}^{N} \Bigg[& \frac{P_i^2(t)}{2M_{\rm eff}} + \frac{1}{2} M_{\rm eff}\ \omega_{\rm CVM}^2 (x_i(t) - x_{0,i})^2 + \\ & - \frac{1}{2} \sum_{\substack{j=1 \\ j\neq i}}^{N} Z_{{\rm eff},i} e x_i(t) \hat{\mathbf{p}}_i \cdot \mathbf{E}_j(\mathbf{r}_i, t) \Bigg] \end{aligned} \tag{56}$$

where $x_{0,i}$ is the distance between charge barycenters, $P_i = M_{\rm eff}\,\dot{x}_i(t)$ is the conjugate variable of the charge barycenter distance x_i and $\mathbf{E}_j(\mathbf{r}_i, t)$ is the electric field generated by the j-th particle at the point $\mathbf{r}_i$ at the time t. In order to derive the equations of motion for the system of coupled dipoles we need to express the electromagnetic field generated by the j-th molecule in terms of the charge barycenter separation x_j. According to Eq.(50) we can consider as fixed the positions and the orientations of the dipoles.

The electric field $\mathbf{E}_i(\mathbf{r},t)$ splits into a static and a dynamic component, i.e.

$$\begin{aligned}\mathbf{E}_i(\mathbf{r},t) &= \mathbf{E}_{\text{stat},i}(\mathbf{r}) + \mathbf{E}_{\text{dyn},i}(\mathbf{r},t) = \mathbf{E}_{\text{stat},i}(\mathbf{r}) + \int_{\mathbb{R}\setminus\{0\}} \mathbf{E}_{\text{dyn},i}(\mathbf{r},\omega)\exp(-\mathrm{i}\,\omega t)\ \mathrm{d}\omega = \\ &= \mathbf{E}_{\text{stat},i}(\mathbf{r}) + \int_{\mathbb{R}^+\setminus\{0\}} 2|\mathbf{E}_{\text{dyn},i}(\mathbf{r},\omega)|\cos\left[\omega t - \theta_E(\omega)\right]\ \mathrm{d}\omega\end{aligned} \tag{57}$$

where the polar representation of the Fourier coefficients of the electromagnetic field has been used; $\mathbf{E}_{\text{stat},i}(\mathbf{r})$ is the static component of the electromagnetic field while $\mathbf{E}_{\text{dyn},i}(\mathbf{r},\omega)$ is the dynamical electric field generated by dipole oscillations. The electric fields generated by static charge distributions are subjected to Debye-Hückel screening due to the freely moving ions on a characteristic length scale λ_D

$$\lambda_D = \left(\frac{\sum_i \rho_{\infty,i} e^2 z_i^2}{\varepsilon_0 \varepsilon_W k_B T}\right)^{-1/2} \tag{58}$$

where $\rho_{\infty,i}$ is the concentration of the i-th electrolyte species and T is the temperature of the solution. In experiments mimicking biological conditions, the ionic strength of the NaCl solution has to be set at 200 mM, which results in a Debye length $\lambda_D \approx 9.74\,\text{Å}$. In this condition, the electrostatic field $\mathbf{E}_{\text{stat},i}(\mathbf{r})$ generated by the i-th charge distribution located at $\mathbf{r}_i$ and characterized by a total charge Z_{Net} and electric dipole $\mathbf{p}_i = p_{0,i}\hat{\mathbf{p}}_i$ is given by [23]:

$$\begin{aligned}\mathbf{E}_{\text{stat},i}(\mathbf{r}) = \frac{\exp[-|\mathbf{r}-\mathbf{r}_i|/\lambda_D]}{4\pi\varepsilon_0\varepsilon_W(0)}\Bigg\{ &\frac{Z_{\text{Net,i}}e}{|\mathbf{r}-\mathbf{r}_i|}\left(\frac{1}{|\mathbf{r}-\mathbf{r}_i|}+\frac{1}{\lambda_D}\right)\hat{\mathbf{n}}_{\mathbf{r}_i\mathbf{r}} + \\ + p_{0,i}\Bigg[&\left(\frac{3}{|\mathbf{r}-\mathbf{r}_i|^3}+\frac{3}{\lambda_D|\mathbf{r}-\mathbf{r}_i|^2}+\frac{1}{\lambda_D^2|\mathbf{r}-\mathbf{r}_i|}\right)(\hat{\mathbf{n}}_{\mathbf{r}_i\mathbf{r}}\cdot\hat{\mathbf{p}}_i)\hat{\mathbf{n}}_{\mathbf{r}_i\mathbf{r}} + \\ - &\left(\frac{1}{|\mathbf{r}-\mathbf{r}_i|^3}-\frac{1}{\lambda_D|\mathbf{r}-\mathbf{r}_i|^2}\right)\hat{\mathbf{p}}_i\Bigg]\Bigg\}\end{aligned} \tag{59}$$

where $\hat{\mathbf{n}}_{\mathbf{r}\mathbf{r}_i} = (\mathbf{r}-\mathbf{r}_i)/|\mathbf{r}-\mathbf{r}_i|$ is the unit vector along the direction joining the dipole and the point $\mathbf{r}$. Assuming a minimal intermolecular average distance among biomolecules to be considered in THz spectroscopy experiments $\langle r\rangle \approx 600\,\text{Å}$, so that in the electrostatic potential the leading term is

$$\mathbf{E}_{\text{stat},i}(\mathbf{r}) \approx \frac{\exp[-|\mathbf{r}-\mathbf{r}_i|/\lambda_D]}{4\pi\varepsilon_0\varepsilon_W(0)\lambda_D|\mathbf{r}-\mathbf{r}_i|}\left[Z_{\text{Net}}e + \frac{p_{0,i}}{\lambda_D}(\hat{\mathbf{n}}_{\mathbf{r}_i\mathbf{r}}\cdot\hat{\mathbf{p}}_i)\right]\hat{\mathbf{n}}_{\mathbf{r}_i\mathbf{r}} = E_{stat,i}(\mathbf{r})\hat{\mathbf{n}}_{\mathbf{r}_i\mathbf{r}} \tag{60}$$

The dynamics of the electromagnetic field is described by D'Alembert equation in Lorenz

gauge reading

$$\left[|\mathbf{k}|^2 - \frac{\omega^2}{v_c^2(\omega)}\right] \mathbf{A}_i(\mathbf{k},\omega) = \mu(\omega)\mathbf{J}_i(\mathbf{k},\omega) \tag{61}$$

where $v_c^2(\omega) = c^2/[\varepsilon_W(\omega)\mu_W(\omega)] = [\varepsilon_0\varepsilon_W(\omega)\mu_0\mu_W(\omega)]^{-1}$ represent the (complex) speed of propagation of light. In our case we can safely assume that the relative magnetic permittivity is 1, i.e. $\mu_W(\omega) = 1$ and the solution in real space is given by

$$\mathbf{A}_i(\mathbf{r},\omega) = \mu_0 \int_{\mathbb{R}^3} \frac{\mathbf{J}_i(\mathbf{k},\omega)}{|\mathbf{k}|^2 - k_0^2(\omega)} \exp[+\mathrm{i}\mathbf{k}\cdot\mathbf{r}] \ \mathrm{d}^3k \tag{62}$$

where $k_0^2(\omega) = \omega^2/v_c^2(\omega) \in \mathbb{C}$. The Fourier components of the current associated to the oscillation of the i-th dipole are

$$\mathbf{J}_i(\mathbf{k},\omega) = \frac{1}{(2\pi)^4}\int_{\mathbb{R}^3} \mathrm{d}^3k \int_{\mathbb{R}} \mathrm{d}\omega \ \ \mathbf{J}_i(\mathbf{r},t)\exp[-\mathrm{i}(\mathbf{k}\cdot\mathbf{r}-\omega t)] = \frac{p_i(\omega)\hat{\mathbf{p}}_i}{(2\pi)^3}(-\mathrm{i}\omega)\exp(-\mathrm{i}\mathbf{k}\cdot\mathbf{r}_i) \tag{63}$$

where

$$\begin{aligned}
&\mathbf{J}_i(\mathbf{r},t) = Z_{\mathrm{eff}}e\left[\dot{r}_{i,+}\delta(\mathbf{r}-\mathbf{r}_{i,+}) - \dot{r}_{i,-}\delta(\mathbf{r}-\mathbf{r}_{i,-})\right]\hat{\mathbf{p}}_i = \frac{Z_{\mathrm{eff}}e\ \hat{\mathbf{p}}_i}{(2\pi)^3}\int_{\mathbb{R}^3}\big[\dot{r}_{i,+}\exp\left(-\mathrm{i}\mathbf{k}\cdot\Delta\mathbf{r}_{i,+}\right) + \\
&- \dot{r}_{i,-}\exp\left(-\mathrm{i}\mathbf{k}\cdot\Delta\mathbf{r}_{i,-}\right)\big]\exp\left[-\mathrm{i}\mathbf{k}\cdot(\mathbf{r}-\mathbf{r}_i)\right] \ \mathrm{d}^3k \approx \frac{Z_{\mathrm{eff}}e\dot{x}_i\ \hat{\mathbf{p}}_i}{(2\pi)^3}\int_{\mathbb{R}^3}\exp\left[-\mathrm{i}(\mathbf{r}-\mathbf{r}_i)\right] \ \mathrm{d}^3k = \\
&= \frac{\dot{p}_i\ \hat{\mathbf{p}}_i}{(2\pi)^3}\int_{\mathbb{R}^3}\exp\left[-\mathrm{i}\mathbf{k}\cdot(\mathbf{r}-\mathbf{r}_i)\right] \ \mathrm{d}^3k = \delta(\mathbf{r}-\mathbf{r}_i)\frac{\mathrm{d}\mathbf{p}_{\mathrm{dyn},i}}{\mathrm{d}t}
\end{aligned} \tag{64}$$

where we have introduced the distance $\Delta\mathbf{r}_{\pm,i} = \mathbf{r}_\pm - \mathbf{r}_i$ of the positive and negative charge barycenters from the center of net charges, and the dipole approximation has been considered, i.e. $\mathbf{k}\cdot\Delta\mathbf{r}_{\pm,i} \ll 1$. Moreover, it has been assumed that the orientation of the dipoles is fixed ($\dot{\hat{\mathbf{p}}}_i = 0$). Under these assumptions it follows that the only source of the electromagnetic field are the oscillating dipoles.

Substituting Eq.(63) in Eq.(62) we obtain

$$\begin{aligned}
\mathbf{A}_i(\mathbf{r},\omega) &= \frac{\mu_0(-\mathrm{i}\omega)p_i(\omega)\hat{\mathbf{p}}_i}{(2\pi)^3}\int_{\mathbb{R}^3}\frac{\exp[\mathrm{i}\mathbf{k}\cdot(\mathbf{r}-\mathbf{r}_i)]}{|\mathbf{k}|^2-k_0^2}\mathrm{d}^3k = \\
&= \frac{\mu_0(-\mathrm{i}\omega)p_i(\omega)\hat{\mathbf{p}}_i}{4\pi|\mathbf{r}-\mathbf{r}_i|}\exp[\varsigma\,\mathrm{i}\,k_0(\omega)|\mathbf{r}-\mathbf{r}_i|] = \\
&= \frac{\mu_0(-\mathrm{i}\omega)p_i(\omega)\hat{\mathbf{p}}_i}{4\pi|\mathbf{r}-\mathbf{r}_i|}\exp[\varsigma\,\mathrm{i}\,\mathrm{Re}(k_0)|\mathbf{r}-\mathbf{r}_i|]\exp[-|\mathrm{Im}(k_0)||\mathbf{r}-\mathbf{r}_i|]
\end{aligned} \tag{65}$$

where $k_0 = \sqrt{k_0(\omega)^2} \in \mathbb{C}$ and $\varsigma = \mathrm{sgn}[\mathrm{Im}(k_0)]$. According to the conventions adopted in Appendix A for the dielectric constant of water $\varsigma = \mathrm{sgn}(\omega)$. Using Maxwell equations, the expressions of the magnetic field is

$$\mathbf{H}_i(\mathbf{r},\omega) = \frac{\mathrm{rot}\mathbf{A}_i(\mathbf{r},\omega)}{\mu_0\mu_W(\omega)} = (\hat{\mathbf{n}}_{\mathbf{r}\mathbf{r}_i} \times \hat{\mathbf{p}}_i)\frac{\varsigma\omega k_0(\omega)p_i(\omega)}{4\pi|\mathbf{r}-\mathbf{r}_i|}\left(1 - \frac{1}{\mathrm{i}\varsigma k_0(\omega)|\mathbf{r}-\mathbf{r}_i|}\right)\exp[\varsigma\,\mathrm{i}\,k_0(\omega)|\mathbf{r}-\mathbf{r}_i|] \tag{66}$$

and of the electric field is

$$\mathbf{E}_i(\mathbf{r},\omega) = \frac{1}{(-i\omega)\varepsilon_0\varepsilon_W(\omega)}\left[\mathrm{rot}\mathbf{H}_i(\mathbf{r},\omega) - \mu_W(\omega)\mathbf{J}_i(\mathbf{r},\omega)\right] \ . \tag{67}$$

The Fourier transform in frequency domain of the dynamical part of the electric field generated by the i-th dipole for $\mathbf{r} \neq \mathbf{r}_i$ reads

$$\begin{aligned}\mathbf{E}_{\mathrm{dyn},i}(\mathbf{r},\omega) =& \frac{p_i(\omega)}{4\pi\varepsilon_0\varepsilon_W(\omega)}\left\{\frac{k_0^2(\omega)}{|\mathbf{r}-\mathbf{r}_i|}(\hat{\mathbf{n}}_{\mathbf{r}\mathbf{r}_i} \times \hat{\mathbf{p}}_i) \times \hat{\mathbf{n}}_{\mathbf{r}\mathbf{r}_i} + \right. \\ &\left. + \left(\frac{1}{|\mathbf{r}-\mathbf{r}_i|^3} - \frac{\mathrm{i}\varsigma k_0(\omega)}{|\mathbf{r}-\mathbf{r}_i|^2}\right)[3(\hat{\mathbf{n}}_{\mathbf{r}\mathbf{r}_i}\cdot\hat{\mathbf{p}}_i)\hat{\mathbf{n}}_{\mathbf{r}\mathbf{r}_i} - \hat{\mathbf{p}}_i]\right\}\exp[\mathrm{i}\varsigma k_0(\omega)|\mathbf{r}-\mathbf{r}_i|] \ .\end{aligned} \tag{68}$$

The attenuation range (by a factor e) of the field is given by $\lambda_{\mathrm{att}}(\omega) = \mathrm{Im}^{-1}[k_0(\omega)]$ while the field wavelength is given by $\lambda(\omega) = 2\pi\mathrm{Re}^{-1}[k_0(\omega)]$. In the NaCl water solution condition to be used in experiments, and in the range of (angular) frequencies ω attributed to the collective oscillations (CVM) of the biomolecules under consideration (R-PA and BSA) it is $\lambda(\omega) \gtrsim 10\lambda_{\mathrm{att}}(\omega)$. It follows that the retardation effects can be neglected, leading to

$$\mathbf{E}_{\mathrm{dyn},i}(\mathbf{r},\omega) = \frac{p_i(\omega)}{4\pi\varepsilon_0\varepsilon_W(\omega)|\mathbf{r}-\mathbf{r}_i|^3}[3(\hat{\mathbf{n}}_{\mathbf{r}\mathbf{r}_i}\cdot\hat{\mathbf{p}}_i)\hat{\mathbf{n}}_{\mathbf{r}\mathbf{r}_i} - \hat{\mathbf{p}}_i] \ . \tag{69}$$

So, the real electric field can be rewritten as

$$\begin{aligned}\mathbf{E}_{\mathrm{dyn},i}(\mathbf{r},t) &= \int_{\mathbb{R}^+/\{0\}} \frac{p_i(\omega)}{4\pi\varepsilon_0\varepsilon_W(\omega)|\mathbf{r}-\mathbf{r}_i|^3}[3(\hat{\mathbf{n}}_{\mathbf{r}\mathbf{r}_i}\cdot\hat{\mathbf{p}}_i)\hat{\mathbf{n}}_{\mathbf{r}\mathbf{r}_i} - \hat{\mathbf{p}}_i]\exp(-\mathrm{i}\omega t)\mathrm{d}\omega = \\ &= \frac{[3(\hat{\mathbf{n}}_{\mathbf{r}\mathbf{r}_i}\cdot\hat{\mathbf{p}}_i)\hat{\mathbf{n}}_{\mathbf{r}\mathbf{r}_i} - \hat{\mathbf{p}}_i]}{4\pi\varepsilon_0|\mathbf{r}-\mathbf{r}_i|^3}\int_{\mathbb{R}^+/\{0\}}\frac{p_i(\omega)\exp(-\mathrm{i}\phi_{\varepsilon_W}(\omega))\exp(-\mathrm{i}\omega t)}{|\varepsilon_W(\omega)|}\mathrm{d}\omega\end{aligned} \tag{70}$$

where we have used $\varepsilon_W(\omega) = |\varepsilon_W(\omega)| \exp[+\mathrm{i}\phi_{\varepsilon_W}(\omega)]$. Using the reality condition on the time dependent dielectric constant $\varepsilon_W(t)$, i.e. $\phi_{\varepsilon_W}(-\omega) = -\phi_{\varepsilon_W}(\omega)$, we obtain

$$\mathbf{E}_{\mathrm{dyn},i}(\mathbf{r},t) = \frac{[3(\hat{\mathbf{n}}_{\mathbf{r}\mathbf{r}_i}\cdot\hat{\mathbf{p}}_i)-\hat{\mathbf{p}}_i]}{4\pi\varepsilon_0|\mathbf{r}-\mathbf{r}_i|^3}\mathcal{P}_i(t)\ , \tag{71}$$

where the effective generating dipole $\mathcal{P}_i(t)$ is defined as

$$\mathcal{P}_i(t) = \int_{\mathbb{R}^+/\{0\}} \frac{2|p_i(\omega)|\cos\left[\omega t-\phi_i(\omega)-\phi_{\varepsilon_W}(\omega)\right]}{|\varepsilon_W(\omega)|^2}\mathrm{d}\omega = \int_{-\infty}^{t}\chi(t-t')p_i(t')\,\mathrm{d}t'\ , \tag{72}$$

and the response function $\chi(t-t')$ depends on the dielectric properties of the water solution. The interaction energy between the i-th dipole and the electric field generated by the j-th dipole $\mathcal{P}_j$ is given by

$$\begin{aligned} V_{\mathrm{dyn},ij} &= \frac{\hat{\mathbf{p}}_i\cdot\hat{\mathbf{p}}_j-3(\hat{\mathbf{p}}_i\cdot\hat{\mathbf{n}}_{\mathbf{r}_i\mathbf{r}_j})(\hat{\mathbf{p}}_i\cdot\hat{\mathbf{n}}_{\mathbf{r}_i\mathbf{r}_j})}{4\pi\varepsilon_0|\mathbf{r}_i-\mathbf{r}_j|^3}\mathcal{P}_j(t)p_i(t) = \\ &= \frac{\hat{\mathbf{p}}_i\cdot\hat{\mathbf{p}}_j-3(\hat{\mathbf{p}}_i\cdot\hat{\mathbf{n}}_{\mathbf{r}_i\mathbf{r}_j})(\hat{\mathbf{p}}_i\cdot\hat{\mathbf{n}}_{\mathbf{r}_i\mathbf{r}_j})}{4\pi\varepsilon_0|\mathbf{r}_i-\mathbf{r}_j|^3}\int_{-\infty}^{t}\mathrm{d}t'\ \chi(t-t')p_j(t')p_i(t)\,. \end{aligned} \tag{73}$$

The dispersion effects do not allow to provide a straightforward Hamiltonian formulation of the dynamics of the oscillating dipoles; for this reason we introduce an effective dipole $\tilde{\mathcal{P}}_i(t) = \mathcal{C}p_i(t)$ with no phase mismatch effects due to the dispersion properties of the aqueous solution, i.e.

$$\sqrt{\langle\mathcal{P}^2\rangle_{[0,+\infty)}} = \sqrt{\langle\tilde{\mathcal{P}}^2\rangle_{[0,+\infty)}} \tag{74}$$

where $\langle\cdot\rangle_{[0,T]}$ stands for the time average on the interval $[0,T]$. The condition in Eq.(74) can be rewritten as

$$\sqrt{\int_0^{+\infty}\frac{2|p_i(\omega)|^2}{|\varepsilon_W(\omega)|^2}\,\mathrm{d}\omega} = \mathcal{C}\sqrt{\int_0^{+\infty}2|p_i(\omega)|^2\,\mathrm{d}\omega} \tag{75}$$

and assuming that the modulus of the complex dielectric constant is almost constant on the support of $|p_i(\omega)|$, centered around ω_{CVM}, we obtain

$$\mathcal{C} = \frac{1}{|\varepsilon_W(\omega_{\mathrm{CVM}})|}\ . \tag{76}$$

We verify that, in the case of study, we can effectively expect that the variation of the modulus of the dielectric constant is negligible. According to what is reported in Appendix

A about the dielectric properties of salty water, we can expect that in conditions analogous to the experimental ones the maximum variation of the modulus of the (complex) dielectric constant is given by

$$\Delta|\varepsilon(\omega)| \approx \left|\frac{\mathrm{d}|\varepsilon(\omega_{\mathrm{CVM}})|}{\mathrm{d}\omega}(\Delta\omega)_{\mathrm{FS}}\right| \tag{77}$$

where $(\Delta\omega)_{\mathrm{FS}}$ is the maximum of the experimentally expected frequency shift of the absorption peak in the THz spectrum of a protein. For R-PE $\mathrm{d}|\varepsilon(\omega_{\mathrm{CVM}})|/\mathrm{d}\omega = -43.6\,\mathrm{ps}$ and $(\Delta\omega)_{\mathrm{FS}} \approx 2.6 \times 10^{-3}\mathrm{THz}$, from which it follows that $(\Delta|\varepsilon(\omega)|)_{\mathrm{RPE}} \approx 1.2 \times 10^{-1}$ and $(\Delta|\varepsilon(\omega)|)_{\mathrm{RPE}}/|\varepsilon(\omega_{\mathrm{CVM}})| \approx 5.1 \times 10^{-3}$. This means that at the level of accuracy expected by the current theoretical interpretation of the possible experimental results, the approximation of a constant absolute value of the dielectric constant is a good one. In the case of BSA we have that $\mathrm{d}|\varepsilon(\omega_{\mathrm{CVM}})|/\mathrm{d}\omega = -1.91\,\mathrm{ps}$ and $(\Delta\omega)_{\mathrm{FS}} \approx 0.81 \times 10^{-1}\mathrm{THz}$; according to Eq.(77) the estimated variation of the modulus of the relative dielectric constant is $(\Delta|\varepsilon(\omega)|)_{\mathrm{RPE}} \approx 1.6 \times 10^{-1}$, whence $(\Delta|\varepsilon(\omega)|)_{\mathrm{RPE}}/|\varepsilon(\omega_{\mathrm{CVM}})| \approx 2.1 \times 10^{-2}$.

From the above considerations, it follows that the potential between oscillating dipoles can be rewritten as

$$\begin{aligned} V_{\mathrm{dyn},ij}(t) &= \frac{\hat{\mathbf{p}}_i \cdot \hat{\mathbf{p}}_j - 3(\hat{\mathbf{p}}_i \cdot \hat{\mathbf{n}}_{\mathbf{r}_i\mathbf{r}_j})(\hat{\mathbf{p}}_i \cdot \hat{\mathbf{n}}_{\mathbf{r}_i\mathbf{r}_j})}{4\pi\varepsilon_0|\varepsilon_W(\omega_{\mathrm{CVM}})||\mathbf{r}_i - \mathbf{r}_j|^3} p_j(t)p_i(t) = \\ &= Z_iZ_je^2\frac{\hat{\mathbf{p}}_i \cdot \hat{\mathbf{p}}_j - 3(\hat{\mathbf{p}}_i \cdot \hat{\mathbf{n}}_{\mathbf{r}_i\mathbf{r}_j})(\hat{\mathbf{p}}_i \cdot \hat{\mathbf{n}}_{\mathbf{r}_i\mathbf{r}_j})}{4\pi\varepsilon_0|\varepsilon_W(\omega_{\mathrm{CVM}})||\mathbf{r}_i - \mathbf{r}_j|^3} x_i(t)x_j(t)\,. \end{aligned} \tag{78}$$

This is the electrodynamic potential between two biomolecules when collective giant dipole oscillation are activated by an external source of energy.

We are now able to describe the dynamics of the hamiltonian system of dipole oscillators. Let us introduce the variables x_{dyn} expressing the dynamical part of the separation between the barycenters of charge , i.e.

$$x_i(t) = x_{\mathrm{eq},i} + x_{\mathrm{dyn},i}(t) = x_{\mathrm{eq},i} + \int_{\mathbb{R}/\{0\}} 2x_i(\omega)\cos[\omega t + \phi_i(\omega)]\ \mathrm{d}\omega \tag{79}$$

where $x_{\mathrm{eq},i}$ is the static equilibrium elongation of the dipole associated with the i-th molecule, i.e.

$$\partial_{x_{\mathrm{dyn},i}} H\big|_{\boldsymbol{x}_{\mathrm{dyn}}=0} = 0 \qquad \forall i = 1, ..., N\ . \tag{80}$$

From Eq.(79) it follows that the canonical conjugate momenta associated to the variables $x_{\mathrm{dyn},i}(t)$ remain unchanged with respect to the momenta P_i associated to the variables x_i.

According to Eqs.(60) and (71), we can rewrite the electric field generated by the i-th molecule using the variables introduced in Eq.(79)

$$\mathbf{E}_i(\mathbf{r},t) = \boldsymbol{\chi}^{(s)}(\mathbf{r};\mathbf{r}_i,\hat{\mathbf{p}}_i)p_{0,i} + \boldsymbol{\chi}^{(d)}(\mathbf{r};\mathbf{r}_i,\hat{\mathbf{p}}_i)p_{\mathrm{dyn},i}(t) \tag{81}$$

where

$$\begin{aligned}
\boldsymbol{\chi}^{(s)}(\mathbf{r};\mathbf{r}_i,\hat{\mathbf{p}}_i) &= \frac{\exp[-|\mathbf{r}-\mathbf{r}_i|/\lambda_D]}{4\pi\varepsilon_0\varepsilon_W(0)\lambda_D|\mathbf{r}-\mathbf{r}_i|}\frac{\hat{\mathbf{n}}_{\mathbf{r}_i\mathbf{r}}}{\lambda_D}(\hat{\mathbf{n}}_{\mathbf{r}_i\mathbf{r}}\cdot\hat{\mathbf{p}}_i) \\
\boldsymbol{\chi}^{(d)}(\mathbf{r};\mathbf{r}_i,\hat{\mathbf{p}}_i) &= \frac{[3(\hat{\mathbf{n}}_{\mathbf{r}\mathbf{r}_i}\cdot\hat{\mathbf{p}}_i)-\hat{\mathbf{p}}_i]}{4\pi\varepsilon_0\varepsilon_W(\omega_{\mathrm{CVM}})|\mathbf{r}-\mathbf{r}_i|^3} \ .
\end{aligned} \tag{82}$$

With the notations introduced in Eqs.(79) and (82) the equations of motions become

$$\begin{cases}
\dot{x}_i = \dfrac{P_i}{M_{\mathrm{eff}}} \\
\dot{P}_i = -M_{\mathrm{eff}}\omega^2_{\mathrm{CVM}}x_{\mathrm{dyn},i} + \dfrac{Z_{\mathrm{eff},i}Z_{\mathrm{eff},j}e^2}{2}\times \\
\times\displaystyle\sum_{\substack{j=1\\j\neq i}}^{N}\left[p_{eq,j}\left(\hat{\mathbf{p}}_i\cdot\boldsymbol{\chi}^{(s)}(\mathbf{r}_i;\mathbf{r}_j,\hat{\mathbf{p}}_j)+\hat{\mathbf{p}}_j\cdot\boldsymbol{\chi}^{(d)}(\mathbf{r}_j;\mathbf{r}_i,\hat{\mathbf{p}}_i)\right)+2p_{\mathrm{dyn},j}\hat{\mathbf{p}}_i\cdot\boldsymbol{\chi}^{(d)}(\mathbf{r}_i;\mathbf{r}_j,\hat{\mathbf{p}}_j)\right]
\end{cases} \tag{83}$$

where we have used $\hat{\mathbf{p}}_i\cdot\boldsymbol{\chi}^{(d)}(\mathbf{r}_i;\mathbf{r}_j,\hat{\mathbf{p}}_j) = \hat{\mathbf{p}}_j\cdot\boldsymbol{\chi}^{(d)}(\mathbf{r}_j;\mathbf{r}_i,\hat{\mathbf{p}}_i)$. As we are interested in the long range behaviour when $|\mathbf{r}_i-\mathbf{r}_j| \gg \lambda_D$ we can neglect terms containing χ^s in Eq.(83). Introducing the geometric coupling parameter $\zeta_{ij} = -\hat{\mathbf{p}}_i\cdot\boldsymbol{\chi}^{(d)}(\mathbf{r}_i;\mathbf{r}_j,\hat{\mathbf{p}}_j)$ we can rewrite the equations of motion for $x_{\mathrm{dyn},i}$ in terms of its Fourier components yielding

$$\begin{aligned}
&\int_{\mathbb{R}/\{0\}}\left\{[-\omega^2+\omega^2_{\mathrm{CVM}}]x_{\omega,i}\cos(\omega t+\phi_{i,\omega})+\sum_{\substack{j=1\\j\neq i}}^{N}\frac{Z_{\mathrm{eff},i}Z_{\mathrm{eff},j}\zeta_{ij}}{M_{\mathrm{eff}}}x_{\omega,j}\cos(\omega t+\phi_{j,\omega})\right\}\ \mathrm{d}\omega+ \\
&+\omega^2_{\mathrm{CVM}}(x_{\mathrm{eq},i}-x_{0,i})+\sum_{\substack{j=1\\j\neq i}}\frac{Z_{\mathrm{eff},i}Z_{\mathrm{eff},j}e^2\zeta_{ij}}{M_{\mathrm{eff}}}x_{eq,j}=0
\end{aligned} \tag{84}$$

The condition for $x_{\mathrm{eq},i}$ can be rewritten as

$$M_{ij}x_{\mathrm{eq},j} = x_{0,i} \qquad \text{with} \quad M_{ij} = \delta_{ij} + \frac{Z_{\mathrm{eff},i}Z_{\mathrm{eff},j}e^2\zeta_{ij}}{M_{\mathrm{eff}}\omega_{\mathrm{CVM}}^2}(1-\delta_{ij}) \tag{85}$$

while the condition for the solutions of the dynamics can be rewritten as a set of equations for the normal modes of the system, i.e.

$$(M_{ij} - \tilde{\omega}^2\delta_{ij})x_{\omega,j} = 0 \tag{86}$$

where $\tilde{\omega} = \omega/\omega_{\mathrm{CVM}}$. The set of eigenvalues of the matrix M defines the square of the angular frequencies of the normal modes $\{\tilde{\omega}_A\}_{A=1,...,N}$. The eigenfrequencies are well defined as $\tilde{\omega}_A^2 > 0$ for all $A = 1, ..., N$ in the perurbative regime, i.e.

$$\left| \frac{Z_{\mathrm{eff},i}Z_{\mathrm{eff},j}e^2\zeta_{ij}}{M_{\mathrm{eff}}\omega_{\mathrm{CVM}}^2} \right| \ll 1 \ . \tag{87}$$

Within this theoretical framework it is possible to provide a prediction for the observable frequency shifts. The Hamiltonian of the system can be rewritten as

$$H_{\mathrm{dipOs}}(\{\mathbf{R}_{ij}\}_{ij}) = H_{\mathrm{eq}}(\{\mathbf{R}_{ij}\}_{ij}) + \sum_{A=1}^{N} \tilde{J}_A\tilde{\omega}_A(\{\mathbf{R}_{ij}\}_{ij})\omega_{\mathrm{CVM}} \approx \sum_{A=1}^{N} \tilde{J}_A\tilde{\omega}_A(\{\mathbf{R}_{ij}\}_{ij})\omega_{\mathrm{CVM}} \ . \tag{88}$$

where $H_{\mathrm{eq}}(\{\mathbf{R}_{ij}\}_{ij})$ is the energy contribution of the static dipoles that we assume to be negligible with respect to the other term representing the contribution of the dynamics of the coupled oscillators. In order to define the interaction energy among dipoles as a function of their relative positions $\mathbf{R}_{ij}$, the energy of the oscillators in the limit of infinite mutual distances is considered. In fact, a parameter $\epsilon = \min_{ij} |\mathbf{R}_{ij}|^{-1}$ representing the inverse of a length scale can be introduced such that $\mathbf{R}_{ij} = \widetilde{\mathbf{R}}_{ij}/\epsilon$ where $\widetilde{\mathbf{R}}_{ij} \geq 1$. It follows that the Hamiltonian describing the energy of the coupled oscillators depends on ϵ and that the case of decoupled oscillators can be obtained in the limit

$$H_{\mathrm{freeOs}} = \lim_{\epsilon \to 0^+} H_{\mathrm{dipOs}}(\widetilde{\mathbf{R}}_{ij}/\epsilon) = \sum_{i=1} J_i\omega_{\mathrm{CVM}} \ .$$

In this framework, the interaction energy is defined as

$$\Delta U_{\rm int} = \int_0^1 \frac{{\rm d}H_{\rm dipOs}}{{\rm d}\epsilon}{\rm d}\epsilon\,. \tag{89}$$

Assuming an adiabatic process ideally connecting the asymptotic state of non-interacting dipoles $\epsilon = 0$ and the state of interacting dipoles $\epsilon = 1$, the action J is an adiabatic invariant, i.e. $J_i \approx J_A|_{\epsilon=0}$. The interaction energy takes the form

$$\Delta U_{\rm int}(\{\mathbf{R}_{ij}\}_{ij}) = \sum_{A=1}^{N} J_A \int_1^{\tilde{\omega}_A} \omega_{\rm CVM}\ {\rm d}\eta_A = \sum_{A=1}^{N} J_A \omega_{\rm CVM}[\tilde{\omega}_A(\{\mathbf{R}_{ij}\}_{ij}) - 1]\,. \tag{90}$$

This form of the interaction energy is the generalization to the case of N oscillating dipoles of the results derived in [5] for a pair of oscillating resonant dipoles. In fact, the frequency shift in a system of two coupled identical oscillating dipoles is given by

$$\tilde{\omega}_{\pm} = 1 \pm \frac{Z_{\rm eff}^2 e^2}{8\pi\varepsilon_0\varepsilon(\omega_{\rm CVM})|\mathbf{R}_{12}|^3 M_{\rm eff}\omega_{\rm CVM}} \tag{91}$$

and, consequently, the interaction energy in that case scales as $|\mathbf{R}_{12}|^{-3}$. In the general case of N interacting dipoles, the frequency shift of each normal mode with respect to the reference frequency $\omega_{\rm CVM}$ is a non trivial function depending on the position of all the particles in the system. For such a reason we performed numerical simulations in order to provide a theoretical explanation of the possible experimental outcomes.

2. Theoretical prediction of the magnitude of frequency shift of the absorption peak in THz spectroscopy experiments

In THz absorption spectroscopy experiments, the external monochromatic reading THz field $\mathbf{E}_{\rm read}(t) = E_{\rm read}(t)\hat{\mathbf{E}}_{\rm read}$ couples with the system of mutually interacting excited oscillating dipoles, i.e.

$$U_{\rm read} = -\mathbf{E}_{\rm read}(t)\cdot\mathbf{p}_{\rm Tot} = E_{\rm read}(t)\sum_{i=1}^{N} Z_i e x_i(t)\left(-\hat{\mathbf{p}}_i\cdot\hat{\mathbf{E}}_{\rm test}\right) = \tag{92}$$

$$E_{\rm read}(t)\sum_{i=1}^{N}\sum_{A=1}^{N}\left(-\hat{\mathbf{p}}_i\cdot\hat{\mathbf{E}}_{\rm test}\right) Z_i e\mathcal{O}_i^A\tilde{x}_{0,A}\cos(\theta_A+\phi_A) = E_{\rm read}(t)\sum_{A=1}^{N}\mathcal{C}_{\rm cpl}(\tilde{\omega}_A)\cos\left[\tilde{\theta}_A(t)+\phi_A\right]$$

where we have used $x_i = \sum_{A=1}^{N} \mathcal{O}_i^A \tilde{x}_A = \sum_{A=1}^{N} \mathcal{O}_i^A \tilde{x}_{0,A} \cos\left[\tilde{\theta}_A(t) + \phi_A\right]$.

We assume that the major contribution to THz absorption in experiments is due to the normal mode maximally coupled with the external probing field, i.e.:

$$\mathcal{C}_{\rm Mcpl}(\{\mathbf{r}_i, \hat{\mathbf{p}}_i\}_i) = \max_A \ |\mathcal{C}_{\rm cpl}(\tilde{\omega}_A)| = |\mathcal{C}_{\rm cpl}(\tilde{\omega}_{\rm Mcpl}(\{\mathbf{r}_i, \hat{\mathbf{p}}_i\}_i))| \tag{93}$$

where $\tilde{\omega}_{\rm Mcpl}$ is the angular frequency of the collective mode with the largest absolute value of dipole-field coupling constant.

In Eq.(93) we stressed that the mode with the maximal coupling constant depends on the (fixed) positions and orientations of the molecules. In order to establish the value of the amplitude of each normal mode $\tilde{x}_{0,A}$ we assume that $\tilde{x}_{0,A} \simeq \tilde{x}_{0,B} \simeq \tilde{x}_0$. The value of the coefficients $\tilde{x}_{0,A}$ has been chosen assuming that $\langle (\Delta x_i)^2 \rangle = \frac{x^2_{\rm CVM}}{2}$, where $x^2_{\rm CVM}$ is the amplitude of the oscillation of the barycenters of electric charge and $\langle \cdot \rangle$ is the time average over a time much larger than the $\nu^{-1}_{\rm CVM}$. Under these hypotheses, we deduce that

$$\begin{aligned} \langle (\Delta x_i)^2 \rangle \ &= \ \sum_{A,B} \mathcal{O}_i^A \mathcal{O}_i^B \tilde{x}_{0,A} \tilde{x}_{0,B} \langle \cos(\tilde{\omega}_A t + \phi_A) \cos(\tilde{\omega}_B t + \phi_B) \rangle = \sum_{A,B} \mathcal{O}_i^A \mathcal{O}_i^B \tilde{x}_{0,A} \tilde{x}_{0,B} \frac{\delta_{A,B}}{2} = \\ &= \ \frac{\tilde{x}_0^2}{2} \sum_A (\mathcal{O}_i^A)^2 = \frac{\tilde{x}_0^2}{2} \end{aligned} \tag{94}$$

where we have used the properties of the orthogonal matrix $\sum_{A=1}^{N} (\mathcal{O}_i^A)^2 = 1$. From Eq.(94) it follows that the total dipole associated to each normal mode is given by

$$\mathcal{C}_{\rm cpl}(\tilde{\omega}_A) = \sum_i (-\hat{\mathbf{p}}_i \cdot \hat{\mathbf{E}}_{\rm read}) Z_i e \mathcal{O}_i^A \sqrt{2} \sigma_i = \sum_i (-\mathbf{p}_{A,i} \cdot \hat{\mathbf{E}}_{\rm read}) \tag{95}$$

where we have introduced the electric dipole moment

$$\mathbf{p}_{A,i} = Z_i e \mathcal{O}_i^A \sqrt{2} \sigma_i \hat{\mathbf{p}}_i \tag{96}$$

as the effective electric dipole amplitude at the frequency $\tilde{\omega}_A$ of the i-th molecule. The (absolute value) of the frequency shift can be defined as

$$\|\Delta\omega\| = \tilde{\omega}_{\mathrm{Mcpl}} - \omega_{\mathrm{CVM}} \ . \tag{97}$$

We can analytically estimate the frequency shift for a system of two oscillating dipoles representing two excited biomolecules with fixed positions and orientations

$$\Delta\omega = \frac{Z_i Z_j e^2}{2M_{\mathrm{eff}}\omega_0} \frac{\left[\hat{\mathbf{p}}_i \cdot \hat{\mathbf{p}}_j - 3\left(\hat{\mathbf{p}}_i \cdot \hat{\mathbf{r}}_{ij}\right)\left(\hat{\mathbf{p}}_i \cdot \hat{\mathbf{r}}_{ij}\right)\right]}{4\pi|\varepsilon_W(\omega_{\mathrm{CVM}})|\varepsilon_0 r_{ij}^3} \ . \tag{98}$$

In preliminary THz spectroscopy experiments on R-PE, a relative frequency shift $\|\Delta\omega(600\,\text{Å})\|/\omega_{\mathrm{RPE,CVM}} \approx 6 \times 10^{-3}$ has been measured. Assuming $|\varepsilon_W(\omega_{RPE})| \approx 22.7$, $M_{\mathrm{eff}} \simeq M_{\mathrm{RPE}}/12 \approx 0.2 \times 10^2$kDa, the geometric factor $|\hat{\mathbf{p}}_i \cdot \hat{\mathbf{p}}_j - 3(\hat{\mathbf{p}}_i \cdot \hat{\mathbf{r}}_{ij})(\hat{\mathbf{p}}_j \cdot \hat{\mathbf{r}}_{ij})| \approx 1$, then the effective electric charge is estimated to be

$$Z \approx \sqrt{\frac{8M_{\mathrm{eff}}\omega_0^2\zeta\pi\varepsilon_W(\omega_0)\varepsilon_0\left(600\,\text{Å}\right)^3}{e^2}} = 1.3 \times 10^3 \tag{99}$$

The spatial power density of energy injection in THz spectroscopy experiments is much smaller than the spatial power density of energy injection in FCS experiments. In fact, if we assume that the strength of the dynamic dipole (and consequently of the interaction) is proportional to the amount of the energy injection rate into the protein, we can expect that the oscillating dipole strength (and the strength of the interaction) is smaller in THz spectroscopy experiments than in FCS experiments. This means that in estimating the mean squared elongation of the dipole σ_i^2 we have to consider a smaller value than the one estimated in (47). Assuming that $\sigma_{\Delta x} \sim 0.5 \times \sigma_{\Delta x,Fc} \approx 0.5\,\text{Å}$ as in the case of R-PE, we derive a value of $p_\omega \approx 5.3 \times 10^3$D to explain the frequency shift observed in preliminary THz experiment.

This value of the estimated oscillating dipole strength seems to contradict the previous assumption of a smaller dipole strength than the one we have evaluated for FCS experiments $|\mathbf{p}| \sim 2900$D. However, in the previous estimation of the frequency shift we have considered only two oscillating dipoles: as the electrodynamic interactions among resonating oscillating dipoles are supposed to be long-range (scaling as r^{-3}), we are underestimating the effect of long range dipole-dipole electrodynamic interactions in a many-body system. So we expect that such a value of the dynamical electric dipole is an overestimation of the real value in

experiments.

In real spectroscopic experiments the situation is different with respect to the ideal two body case because the number of R-PE molecules contained in a typical observation volume ($\approx 1\,\mu$L) is of the order $10^{15} - 10^{18}$. So, numerical simulations have been performed in order to investigate how the frequency shift of the absorption peak depends on the intermolecular average distance for a system of interacting dipoles, with fixed positions and orientations, linearly coupled through a quasi-static dipole-dipole potential.

We assume that the testing field of the experiments is linearly polarized along the $\hat{z}$ direction, so that the normal mode of the system that maximizes the coupling with the reading field is the one having the largest polarization along the z-axis. It follows that the relative frequency shift $\Delta\omega = \Delta\omega(\{\hat{\mathbf{p}}_i, \mathbf{r}_i\}_i)$ associated to a given configuration for the position and orientations of the system of dipoles is given by

$$\Delta\omega(\{\hat{\mathbf{p}}_i, \mathbf{r}_i\}_i) = 1 - \sqrt{\omega^2_{max}} \qquad \tilde{\omega}^2_{max} = \{\tilde{\omega}^2_A \,|\, |\mathcal{C}_{\rm cpl}(\tilde{\omega}_A)| = \max_{B=1,\dots,N}\{|\mathcal{C}_{\rm cpl}(\tilde{\omega}_B|\}\}\,. \tag{100}$$

In order to compare the result of numerical simulations with the expected outcomes of THz spectroscopy experiments:

- the average over many configurations of the positions and the orientations of the dipoles has to be considered in order to take into account the thermal and statistical fluctuations of the orientations and positions;
- the average frequency shift for a fixed intermolecular average distance has to be calculated for systems of different size and *extrapolated for large* N, as finite size effects affect systems with long range interactions.

In the following section the protocol to calculate the average over the configurations and to extrapolate the frequency shift for large N is discussed.

B. Algorithm for numerical simulations

The aim of the simulations is to estimate the frequency shift for an ensemble of N spherical molecules of radius a in a cubic box of size L as a function of the intermolecular average distance $\langle d\rangle$. The system of oscillating dipoles consists of three different sets of degrees of

freedom: the coordinates of the center of mass of each particle, the orientation of the main dipole and the coordinate which describes the vibration of the dipole. For each fixed value of the intermolecular average distance $\langle d \rangle$, $n_{CMconf} = 5 \times 10^3$ configurations of the ensemble of molecules have been randomly chosen. The position of the center of each molecule has been randomly set with a uniform probability distribution inside the box, avoiding the overlaps. The orientation of each dipole is described by a couple of polar angular coordinates (θ, ϕ) such that $\theta_i \in [0, \pi)$ and $\phi_i = [0, 2\pi)$ for $i = 1, ..., N$. For each fixed configuration of the centers of mass of the molecules, the orientational degrees of freedom of the molecules have been thermalized using a Monte Carlo-Metropolis scheme. All the trial configurations for the orientations have been generated by adding to the angular coordinates of each particle a randomly chosen number with a uniform distribution. The intervals are $[-\eta\pi, \eta\pi]$ for the θ_i angles and $[-2\eta\pi, 2\eta\pi]$ for the ϕ_i angles. In the performed simulations the parameter that describes the width of the interval has been set to $\eta = 7.5 \times 10^{-3}$. For each configuration of the centers of mass, $n_{therm} = 2 \times 10^3$ Monte Carlo steps have been performed to thermalize the orientations of the dipoles of the system. Then, starting from the final configuration so obtained, an average value of the frequency shift has been computed over $n_{MCstep} = 50$ configurations furtherly generated and interspersed with 10 Monte Carlo steps. The relative frequency shift associated to each intermolecular average distance has been computed as the overall average on a total number of $n_{totsamp} = n_{MCstep} \times n_{CMconf} = 2.5 \times 10^5$ different configurations of the dipole orientations and of the positions of the centers of mass. The potential energy dependence among different configurations has been calculated using the time average of Eq.(78) assuming $x_i(t) = x_{\rm CVM} \cos(\omega_{\rm CVM} t)$.

C. Numerical results

The numerical simulations were performed for systems of different sizes and different values of the dipole moment p_i and of the effective charge Z_i. The entries of the matrix M_{ij} depend on the value of the effective charge and only indirectly on the value of the modulus of the dipole moment of each molecule. The value of the dynamic electric dipole of each molecule enters in the calculation of the total interaction energy among the dipoles required by Monte Carlo-Metropolis algorithm. The tested values of the effective charge were empirically chosen in order to provide a relative frequency shift comparable with the

one observed in preliminary experimental tests. The value of the amplitude of the dynamic dipole oscillations has been chosen heuristically in order to reproduce the same data.

The average frequency shift for a fixed intermolecular average distance has been measured for different sizes of the system. For each fixed number of molecules the relative frequency shift $\Delta\nu_0/\nu_0$ has been plotted as a function of the intermolecular average distance $\langle d\rangle$. The data have been fitted with a power law of the form $\Delta\nu_0/\nu_0 = Ax^{-k}$ and an inverse cubic law $\Delta\nu_0/\nu_0 = Bx^{-3}$.

In conclusion, the highly remarkable result of our computations is that the frequency shift of the collective intramolecular oscillations of an ensemble of proteins interacting through a dipole-dipole electrodynamic force, scales as $1/\langle d\rangle^3$. By inversion, the experimental observation of this result is a proof that the molecules under investigation interact through the electrodynamic dipole-dipole forces above discussed.

N	$A[10^6\ \text{Å}^3]$	k	$B[10^6\ \text{Å}^3]$
50	2.04 ± 0.04	2.65 ± 0.05	1.79 ± 0.04
100	1.438 ± 0.014	2.90 ± 0.02	1.38 ± 0.10
200	1.17 ± 0.02	$k = 3.03 \pm 0.04$	1.185 ± 0.005

TABLE II: Table of the fitted parameters for the relative frequency shift as a function of the intermolecular average distance $\langle d\rangle$ and different system sizes (the number of molecules in the box is N). The parameters $\{A_N, k_N\}_N$ correspond to the fit $\Delta\nu_0/\nu_0 = A_N x^{-k_N}$ and $\{B_N\}_N$ are the parameters characterizing the inverse cubic distribution $\Delta\nu_0/\nu_0 = B_N x^{-3}$. The modulus of each dipole was chosen to be $p_i = 2100$ D while the effective charge of the dipole is $Z_i = 850$. With these choices the amplitude of dipole oscillation is $x_{\omega_0} \simeq 0.51$ Å.

N	$A[10^6\ \text{Å}^3]$	k	$B[10^6\ \text{Å}^3]$
50	1.55 ± 0.02	2.67 ± 0.04	1.37 ± 0.03
100	1.10 ± 0.010	2.95 ± 0.02	1.081 ± 0.005
200	0.907 ± 0.009	3.05 ± 0.02	9.27 ± 0.04

TABLE III: Table of the fitted parameters for the relative frequency shift as a function of the intermolecular average distance $\langle d\rangle$ and different system sizes (the number of molecules in the box is N). The parameters $\{A_N, k_N\}_N$ correspond to the fit $\Delta\nu_0/\nu_0 = A_N x^{-k_N}$ and $\{B_N\}_N$ are the parameters characterizing the inverse cubic distribution $\Delta\nu_0/\nu_0 = B_N x^{-3}$. The modulus of each dipole was chosen to be $p_i = 1850$ D while the effective charge of the dipole is $Z_i = 750$. With these choices the amplitude of dipole oscillation is $x_{\omega_0} \simeq 0.51$ Å.

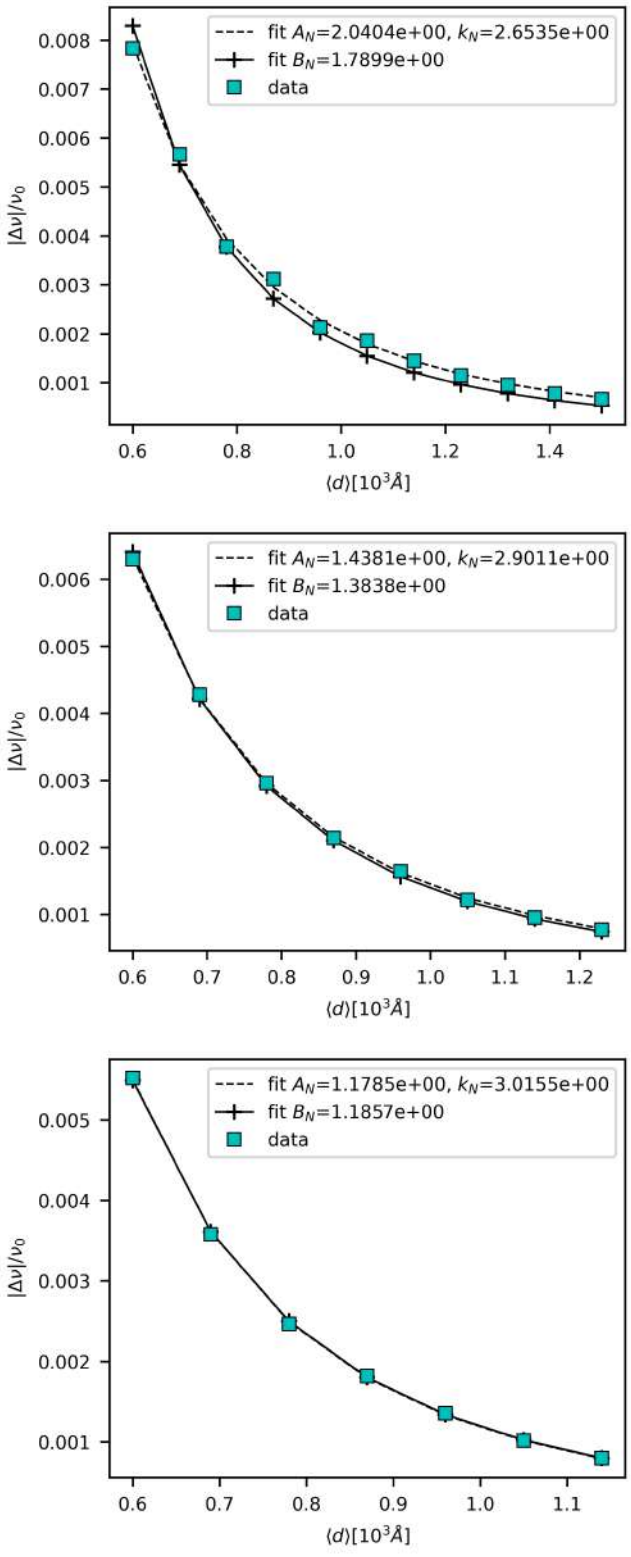

FIG. 10: Relative frequency shift as a function of the intermolecular average distance for N = 50 (top), N = 100 (center) N = 200 (bottom). The coefficients A_N and B_N are expressed in 10^6Å^3. The modulus of each dipole was chosen to be $p_i = 2100\ D$ while the effective charge of the dipole is $Z_i = 850$. With these choices the amplitude of dipole oscillation is $x_{\omega_0} \simeq 0.51\text{Å}$.

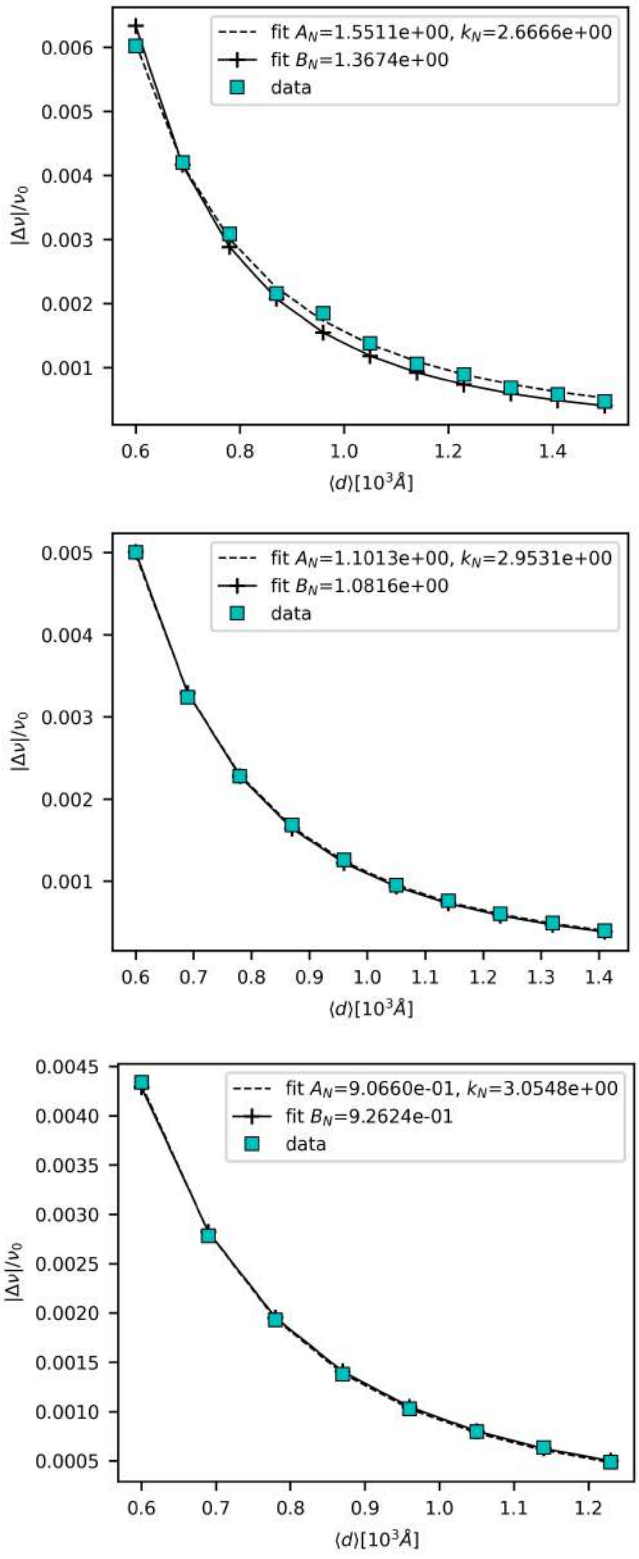

FIG. 11: Relative frequency shift as a function of the intermolecular average distance for N = 50 (top), N = 100 (center) N = 200 (bottom). The coefficients A_N and B_N are expressed in 10^6Å^3. The module of each dipole was chosen to be $p_i = 1850\ D$ while the effective charge of the dipole is $Z_i = 750$. With these choices the amplitude of dipole oscillation is $x_{\omega_0} \simeq 0.51\,\text{Å}$.

IV. REMARK ON POSSIBLE ACTIVATION MECHANISMS OF ELECTRODYNAMIC FORCES IN VIVO

The light-induced activation of electrodynamic forces is expected to be a method to warrant a well controllable and reproducible *in vitro* approach. Even though the R-PE protein is a natural light harvesting protein, we might wonder which kind of activation mechanisms might be hypothesised to take place in living cells. A comment on this point is not out of place because there is no physical reason to consider the activation of electrodynamic forces limited to the creation of "hot points" through the excitation of fluorophores. In fact, the theoretical modelling in Ref.[11] requires an external source of energy injection into a macromolecule of absolutely generic form.

Actually, in vivo the external energy supply for the activation of electrodynamic attractive forces between cognate partners could be well provided by the cellular machinery itself as energy released by adenosine triphosphate (ATP) or guanosine triphosphate (GTP) hydrolysis by specific enzymes. It could then be transferred in the form of post-translational modifications or heat to the other molecules. In fact, the typical intracellular concentration of ATP molecules is given around 1 mM implying that a protein molecule in the cell undergoes around 10^6 collisions with ATP molecules per second [24]. Given the standard free-energy obtained from ATP hydrolysis estimated around 50 kJ $mol^{-1} = 8.306 \cdot 10^{-13}$erg, we can assume that 1% of the collisions with ATP will provide energy, which corresponds to a power supply of $8.306 \cdot 10^{-9}$erg s^{-1} potentially available. Besides ATP hydrolysis, other possible forms of energy supply should be considered in a cellular environment, for example, the energy released from mitochondria in the course of citric acid cycle with a power supply given around 10^{-7}erg s^{-1}. This source of energy might well be enough to excite long-range electrodynamic forces as the corresponding power is around or larger than the power considered for ATP hydrolysis. Let us also mention the recent experimental evidence for thermally induced "protein quakes" to initiate enzymatic catalysis [25] through a solvent-dependent non isotropic momentum transfer due to the collisions of water molecules or ions.

It is worth mentioning that, for a broad class of physical systems, long-living Quasi Stationary States (QSS) can be dynamically generated which keep a system out of thermodynamic equilibrium. Among many other systems where QSS are produced [26] let us mention a beam of fast particles interacting with the set of waves describing a physical

system [27, 28] a situation which is reminiscent, for example, of fast phosphate groups - produced by ATP hydrolysis - colliding against suitable sites of a biomolecule to create "hot points" yielding "protein quakes". In Ref. [11] "protein quakes" have been invoked to explain the activation of collective oscillations through light irradiation of the BSA protein.

Appendix A: Dielectric properties of solution of salt in water

From data reported in [29] we have interpolated the complex dielectric constant of water solution of NaCl at 200 mM at $T = 30\,^{\circ}\mathrm{C}$:

$$\varepsilon_W(\omega) = \varepsilon_{W,\infty} + \frac{\varepsilon_W(0) - \varepsilon_{W,\infty}}{1 - i\omega\tau_W} \tag{A1}$$

with $\varepsilon_{W,\infty} = 5$, $\varepsilon_W(0) = 72.7$ and $\tau = 7.01\,\mathrm{ps}$. It follows that for R-PE ($\omega_{\mathrm{CVM}} = 2\pi \times 71\,\mathrm{GHz} = 0.446\,\mathrm{THz}$) the value of the electric dielectric constant is

$$\varepsilon_W(\omega_{\mathrm{CVM}}) = 11.3 + \mathrm{i}\ 19.6 \tag{A2}$$

so that the characteristic wavelength corresponding to the angular frequency of the CVM observed for the R-PE is

$$k(\omega_{\mathrm{CVM,RPE}}) = (6.13 + \mathrm{i}\ 3.55)\times 10^{-7}\,\mathrm{\AA}^{-1} \tag{A3}$$

assuming $\mu_W(\omega_{\mathrm{CVM}}) = 1$.

	$\varepsilon_W(\omega_{\mathrm{CVM}})$	$\lvert\varepsilon_W(\omega_{\mathrm{CVM}})\rvert$	$\phi_{\varepsilon_W}(\omega_{\mathrm{CVM}})$	$\varepsilon'_W(\omega_{\mathrm{CVM}})$	$\lvert\varepsilon_W(\omega_{\mathrm{CVM}})\rvert'$	$\phi'_\varepsilon(\omega_{\mathrm{CVM}})$
R-PE	$11.3 + \mathrm{i}\,19.6$	22.6	1.050	$-(25.5 + \mathrm{i}35.8)$	-43.8	0.189
BSA	$5.35 + \mathrm{i}\,4.87$	7.24	0.738	$-(0.35 + \mathrm{i}\,2.44)$	-1.91	-0.217

TABLE IV: Dielectric properties of water in the regime of frequency of the Collective Vibration Mode (CVM) for R-PE and BSA. The Fourier transform of the relative dielectric constant of water is expressed using polar form $\varepsilon_W(\omega) = |\varepsilon_W(\omega)|\exp[\mathrm{i}\phi_{\varepsilon_W}(\omega)]$. The derivatives (primed quantities) of the different adimensional quantities with respect to ω are expressed in $\mathrm{ps} = \mathrm{THz}^{-1}$.

An analogous calculation for BSA ($\omega_{\mathrm{CVM}} \simeq 2\pi \times 0.314\,\mathrm{THz} = 1.97\,\mathrm{THz}$) gives $\varepsilon_W(\omega_{\mathrm{CVM,BSA}}) = 5.35132 - \mathrm{i}\ 4.8655$, and the wavenumber is

$$k(\omega_{\mathrm{CVM,BSA}}) = (1.65 - \mathrm{i}\ 0.638)\times 10^{-6}\,\mathrm{\AA}^{-1} \tag{A4}$$

For the biomolecules considered, BSA and R-PE, the characteristic attenuation length scale $\kappa_{\rm att} = [\Im(k)]^{-1}$ is smaller than both the wavelength $\lambda_{\rm rad} = [\Re(k)]^{-1}$ of the radiation and the characteristic length scale of the observed systems in THz spectroscopy experiments, i.e. $l_{\rm sys} \approx (1\,\mu{\rm L})^{1/3} = 10^7 \text{Å} = 10^{-1}{\rm cm}$.

	$\omega_{\rm CVM}$[THz]	$\lambda_{\rm rad}(\omega_{\rm CVM})[\times 10^7 \text{Å}]$	$\kappa_{\rm att}(\omega_{\rm CVM})[\times 10^7 \text{Å}]$	$\kappa^3_{\rm att}[\mu{\rm L}]$
R-PE	0.447	1.02	0.281	0.022
BSA	1.97	0.606	0.156	0.0038

This means that the dissipative properties of the medium define the range of the interaction: inside a volume of $\kappa^3_{\rm att}$ the dynamical electric field can be considered quasi-static, i.e. retardation and radiation terms in Eq.(68) can be neglected.

Appendix B: Effective mass for two oscillating charge centers

Here we consider the inner dynamics of a unidimensional oscillator along a fixed axis. Charge barycenters coordinates $x_\pm$ can be expressed in terms of the relative/center-of-mass coordinates $r = x_+ - x_-$ and $R = (m_+x_+ - m_-x_-)/m_{Tot}$, where $m_{Tot} = m_+ + m_-$ is the total mass of the oscillating dipole. The following assumptions have been made:

- the two charge barycenters are associated to the same effective mass m_+ and m_-;
- the equilibrium position of the system is supposed to correspond to the situation where the two charge barycenters overlap, i.e. $x_+ = x_- = 0$

$$H_{intOsc} = \frac{1}{2}m\dot{x}_+^2 + \frac{1}{2}m\dot{x}_-^2 + \frac{1}{2}m\omega^2(x_+ - R)^2 + \frac{1}{2}m\omega^2(x_- - R)^2 \tag{B1}$$

After the change of coordinates $x_\pm = R \pm r/2$, Eq.(B1) reads:

$$\begin{aligned} H_{intOsc} &= \frac{1}{2}(2m)\dot{R}^2 + \frac{1}{2}\frac{m}{2}\dot{r}^2 + \frac{1}{2}\frac{m}{2}\omega^2 r^2 = \\ &= \frac{1}{2}m_{Tot}\dot{R}^2 + \frac{1}{2}m_{red}\dot{r}^2 + \frac{1}{2}m_{red}\omega^2 r^2 \end{aligned} \tag{B2}$$

Ignoring the contribution to the total energy of the center of mass ($R = 0$, $\dot{R} = 0$), we find that the energy contribution deriving from oscillations reduces to

$$H_{intOsc} = \frac{1}{2}m_{red}\dot{r}^2 + \frac{1}{2}m_{red}\omega^2 r^2\,. \tag{B3}$$

For the protein R-PE, we have that $m_{Tot} \sim 2.4 \times 10^2$ KDa, so that $m_{red} = m/2 = m_{Tot}/4 \approx 0.6 \times 10^2$ KDa.

Acknowledgements

The project leading to this publication has received funding from the Excellence Initiative of Aix-Marseille University - A*MIDEX, a French "Investissements d'Avenir" programme. This work was also partially supported by the Seventh Framework Programme for Research of the European Commission under FET-Proactive grant TOPDRIM (FP7-ICT-318121). Matteo Gori thanks the financial support of DARPA (USA) for his long term visit at Howard University at Washington D.C.

---

[1] Fröhlich, H. Long-range coherence and energy storage in biological systems. *International Journal of Quantum Chemistry* **2**, 641– 649 (1968).

[2] Fröhlich, H. Long range coherence and the action of enzymes. *Nature* **228**, 1093 (1970).

[3] Fröhlich, H. Selective long range dispersion forces between large systems. *Physics Letters A* **39**, 153–154 (1972).

[4] Fröhlich, H. Long-range coherence in biological systems. *Rivista Nuovo Cimento* **7**, 399 – 418 (1977).

[5] Preto, J., Pettini, M. & Tuszynski, J. A. Possible role of electrodynamic interactions in long-distance biomolecular recognition. *Phys. Rev. E* **91**, 052710 ((2015)).

[6] Preto, J., Floriani, E., Nardecchia, I., Ferrier, P. & Pettini, M. Experimental assessment of the contribution of electrodynamic interactions to long-distance recruitment of biomolecular partners: Theoretical basis. *Phys. Rev. E* **85**, 041904 (2012).

[7] Nardecchia, I., Gori, M., Floriani, E., Pettini, M. & et al. Experimental detection of long-distance interactions between biomolecules through their diffusion behavior: Numerical study. *Phys. Rev. E* **90**, 022703 (2014).

[8] Gori, M., Donato, I., Floriani, E., Nardecchia, I. & Pettini, M. Random walk of passive tracers among randomly moving obstacles. *Theoretical Biology and Medical Modelling* **13**, 13 (2016).

[9] Olmi, S., Gori, M., Donato, I. & Pettini, M. Collective behavior of oscillating electric dipoles. *Scientific Reports* **8**, 15748 (2018).

[10] Nardecchia, I., Lechelon, M., Gori, M., Pettini, M. & et al. Detection of long-range electrostatic interactions between charged molecules by means of fluorescence correlation spectroscopy. *Phys. Rev. E* **96**, 022403 (2017).

[11] Nardecchia, I., Gori, M., Sturgis, J., Pettini, M. & et al. Out-of-equilibrium collective oscillation as phonon condensation in a model protein. *Phys. Rev. X* **8**, 031061 (2018).

[12] Richards, F. M. Areas, volumes, packing, and protein structure. *Annual review of biophysics and bioengineering* **6**, 151–176 (1977).

[13] Durchschlag, H. Determination of the partial specific volume of conjugated proteins. *Colloid and Polymer Science* **267**, 1139–1150 (1989).

[14] Chavanis, P.-H. Phase transitions in self-gravitating systems: Self-gravitating fermions and hard-sphere models. *Physical Review E* **65**, 056123 (2002).

[15] Buschmann, V., Krämer, B., Koberling, F., Macdonald, R. & Rüttinger, S. Quantitative fcs: determination of the confocal volume by fcs and bead scanning with the microtime 200. *Application Note PicoQuant GmbH, Berlin* (2009).

[16] Likhachev, E. Dependence of water viscosity on temperature and pressure. *Technical Physics* **48**, 514–515 (2003).

[17] Israelachvili, J. N. *Intermolecular and surface forces* (Academic press, 2011).

[18] Farnum, M. & Zukoski, C. Effect of glycerol on the interactions and solubility of bovine pancreatic trypsin inhibitor. *Biophysical journal* **76**, 2716–2726 (1999).

[19] Lund, M. & Jönsson, B. A mesoscopic model for protein-protein interactions in solution. *Biophysical Journal* **85**, 2940–2947 (2003).

[20] Zhang, Z., Agarwal, G. S. & Scully, M. O. Quantum fluctuations in the fröhlich condensate of molecular vibrations driven far from equilibrium. *Physical Review Letters* **122**, 158101 (2019).

[21] Faraji, E., Franzosi, R., Mancini, S. & Pettini, M. Exciting out-of-equilibrium states in macromolecules through light pumping. *Scientific Reports* **11**, 6591 (2021).

[22] Torshin, I. Y. & Harrison, R. W. Charge centers and formation of the protein folding core. *Proteins* **43**, 353–364 ((2001)).

[23] Tsonchev, S., Schatz, G. C. & Ratner, M. A. Screened multipole electrostatic interactions at the debye–hückel level. *Chem. Phys. Lett.* **400**, 221–225 ((2004)).

[24] Alberts, B. *et al. Molecular Biology of the Cell 4th Edition: International Student Edition* (Routledge, 2002).

[25] Zaragoza, J. P. T. *et al.* Detecting and characterizing the kinetic activation of thermal networks in proteins: Thermal transfer from a distal, solvent-exposed loop to the active site in soybean lipoxygenase. *The Journal of Physical Chemistry B* **123**, 8662–8674 (2019).

[26] Campa, A., Dauxois, T. & Ruffo, S. Statistical mechanics and dynamics of solvable models with long-range interactions. *Physics Reports* **480**, 57–159 (2009).

[27] Barré, J., Dauxois, T., De Ninno, G., Fanelli, D. & Ruffo, S. Statistical theory of high-gain free-electron laser saturation. *Physical Review E* **69**, 045501 (2004).

[28] Carlevaro, N. *et al.* Beam–plasma instability and fast particles: the lynden-bell approach. *Plasma Physics and Controlled Fusion* **56**, 035013 (2014).

[29] Shcherbakov, V., Artemkina, Y. M. & Korotkova, E. Dielectric properties and high-frequency conductivity of the sodium chloride-water system. *Russ. J. Inorg. Chem.* **59**, 922–926 ((2014)).